ESAIM: M2AN 54 (2020) 1073–1109
https://doi.org/10.1051/m2an/2019087

ESAIM: Mathematical Modelling and Numerical Analysis
www.esaim-m2an.org

COMPUTATION OF THE MAGNETIC POTENTIAL INDUCED BY A COLLECTION OF SPHERICAL PARTICLES USING SERIES EXPANSIONS

Stéphane Balac[1,*], Laurent Chupin[2] and Sébastien Martin[3]

Abstract. In Magnetic Resonance Imaging there are several situations where, for simulation purposes, one wants to compute the magnetic field induced by a cluster of small metallic particles. Given the difficulty of the problem from a numerical point of view, the simplifying assumption that the field due to each particle interacts only with the main magnetic field but does not interact with the fields due to the other particles is usually made. In this paper we investigate from a mathematical point of view the relevancy of this assumption and provide error estimates for the scalar magnetic potential in terms of the key parameter that is the minimal distance between the particles. A special attention is paid to obtain explicit and relevant constants in the estimates. When the "non-interacting assumption" is deficient, we propose to compute a better approximation of the magnetic potential by taking into account pairwise magnetic field interactions between particles that enters in a general framework for computing the scalar magnetic potential as a series expansion.

Mathematics Subject Classification. 65N15, 41-04, 78A30, 92C55.

Received July 15, 2019. Accepted December 2, 2019.

1. Introduction

This work is devoted to the study of a way of computing the magnetic field induced by a cluster of metallic particles subjected to the static magnetic field of a Magnetic Resonance Imaging (MRI) device. These magnetic particles locally induce magnetic field inhomogeneities. In some context, magnetic field inhomogeneities are annoying since they perturb the imaging process giving rise to susceptibility artifacts in the image [2, 27]. In other contexts, the magnetic field inhomogeneities induced by the metallic particles can be exploited in the imaging process for medical diagnostic. For instance, in stem cell therapy, magnetic particles are used for the magnetic labeling of cells and MRI offers the potential of tracking these labeled cells *in vivo* [23]. Tumor cell detection can be achieved by labeling the cells with iron oxide-based contrast agents [29]. We can also quote the measurement of susceptibility effects due to blood in brain micro-vessel networks and application to the MRI studies with or without contrast agents [5, 13]. As well, pathological iron deposit in the brain plays a role in neuro-degeneration [31] and iron has been identified as a potential MRI biomarker for early detection

Keywords and phrases. Series expansion, error estimates, Spherical Surface Harmonics, Green's representation formula, magnetic potential, Magnetic Resonance Imaging.

[1] UNIV. RENNES, CNRS, IRMAR – UMR 6625, F-35000 Rennes, France.
[2] LMBP, Université Clermont Auvergne, CNRS UMR 6620, Campus des Cézeaux, 63177 Aubière, France.
[3] Laboratoire MAP5, Université Paris Descartes, CNRS UMR 8145, 45 rue des Saints-Pères, 75270 Paris, France.
*Corresponding author: stephane.balac@univ-rennes1.fr

and diagnosis of Alzheimer's disease. Thus, mapping the brain iron content, identifying and quantifying iron deposits using MRI could provide new ways of diagnosing Alzheimer's disease at an early stage [9]. This list of examples is not exhaustive.

Over the years, numerical simulation has become an essential tool in the research field of MRI, for a better insight into the physical mechanisms that govern the MR signal, for improvement of simulation sequences and protocols, for safety assessment of medical devices, etc. The above mentioned problem is however tricky from a numerical simulation point of view. Indeed, the large amount of particles prevent the use of standard numerical approaches such as the Finite Difference Method [17], the Finite Element Method [12] or methods based on integral formulations [28] since they require the meshing of the computational domain, taking into account metallic inclusions, which is prohibitive from a computational point of view. For such a problem, in the existing MRI literature, the calculation of the variations of the static magnetic field is usually done by adding the analytical solutions of the magnetic field due to sources described by simple geometrical shapes: point sources, spheres, (infinite) cylinders. The simplifying assumption is that the field due to each source interacts only with the main magnetic field but does not interact with the fields due to the other sources, see *e.g.* [3,14,15,21,32] and references therein. This assumption is referred as the "non-interacting assumption". Sometimes, these analytical models are coupled with statistical methods [30] or Monte-Carlo methods [3].

A rather close situation is found in electrostatics for the computation of the electric field due to multiple charged dielectric spheres as encountered in various applications in sciences and engineering such as composite materials, cloud formation, crystalization of charged colloidal, protein folding etc. Numerical methods such as the Boundary Integral Equation Method combined with the Fast Multipole Method [18], the Method of Images [4, 22] or the Method of Moments as well as hybrid methods [10] have been widely investigated and compared in this context.

One of the goals of the present work is to study from a mathematical point of view the validity of the "non-interacting assumption". At best, the assumption is justified experimentally in the above mentioned references. Intuition suggests that this assumption is fulfilled when the particles are "far enough" but that it is defective when the particles are "close" to each other. We quantify in this study how "far" and "close" have to be interpreted.

The features of the particles involved in the above mentioned applications are generally not known precisely. Their shape and size can vary around a mean configuration. However, in order to simplify the mathematical investigations, we assume that all the particles have the same shape and size corresponding to the mean configuration. Namely, we denote by $\Omega_1, \dots, \Omega_N$ the open sets corresponding to the particles, see Figure 1. For simplicity and clarity, we assume that the particles are spherical, *i.e.* the open set Ω_j, $j \in \{1, \dots, N\}$, is a ball centered at position $c_j \in \mathbb{R}^3$. We also assume that all the balls have the same radius denoted by $\varepsilon > 0$. The boundary of Ω_j is denoted by Σ_j. It corresponds to the sphere centered in c_j with radius ε. We also denote by Ω^c the surrounding area, *i.e.* $\Omega^c = \mathbb{R}^3 \setminus \bigcup_{j=1}^N \overline{\Omega_j}$, and by Σ the boundary of Ω^c, *i.e.* $\Sigma = \bigcup_{j=1}^N \Sigma_j$. In this study, besides ε, a key parameter is the minimal distance between two particles defined as

$$\delta = \min_{\substack{i,j\in\{1,\dots,N\}\\ i\neq j}} |c_i - c_j|. \tag{1.1}$$

Moreover, we denote by $R > 0$ the radius of a ball containing all the particles. Assuming the particles are not in contact to each other and using volume considerations, we have the following constraints:

$$\delta > 2\varepsilon \quad \text{and} \quad N\delta^3 < 8R^3. \tag{1.2}$$

We also assume that the particles are made of the same paramagnetic or weak ferromagnetic material and we denote by $\mu_p > 1$ their relative magnetic permeability.

As mentioned earlier, the effect of the main static magnetic field $\mathbf{H_0}$ of the MRI device (assumed to be constant in direction and strength in the area where the particles are located, as it is usually the case in MRI) is to generate a secondary magnetic field induced by the metallic particles. As usual in magneto-statics, the mathematical problem can be formulated in term of the scalar magnetic potential φ.

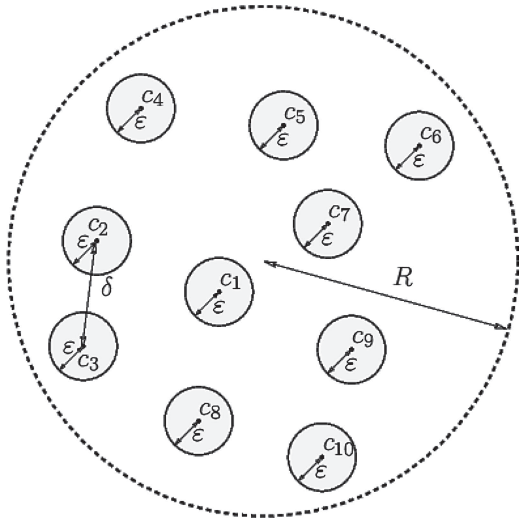

FIGURE 1. Notations used to describe the cluster of metallic particles.

Our first result states that the error made when approaching the magnetic potential φ by the sum of the magnetic potential φ_{c_j} induced by the particles $\Omega_j, j \in \{1, \ldots, N\}$ taken individually, *i.e.* under the "non-interacting assumption", satisfies the following estimate

$$\Big\|\varphi - \sum_{j=1}^{N} \varphi_{c_j}\Big\|_{\mathbb{W}^1(\mathbb{R}^3)} \leqslant 4\sqrt{\pi}\,\frac{(\mu_p - 1)^2}{\mu_p + 2} N \left(\frac{\varepsilon}{R}\right)^{\frac{3}{2}} \left(\frac{2\varepsilon}{\delta}\right)^3 \left(B_3 + 3\ln\left(\frac{2R}{\delta}\right)\right) R\,|\mathbf{H_0}|,$$

where the constant B_3 was found to be $B_3 = 142 + 3\ln 2 \approx 144.1$, see Theorem 3.3. This result is consistent with intuition: when considering a very large number of particles able to fill the area of interest completely and evenly, the ratio $\left(\frac{2\varepsilon}{\delta}\right)^3$ is proportional to the volume fraction of particles. Thus, when the volume fraction is low, that is to say when the particles are spaced at a fairly large distance from each other, computing the magnetic potential by neglecting magnetic field reciprocal interactions between particles gives a quite accurate approximation. Using an integral representation of the error, we also obtain an $\mathbb{L}^\infty$-bound for this error, see Theorem 3.6.

Another goal of the paper is to investigate the more accurate approach where mutual magnetic interactions between metallic particles are also taken into account through a series expansion according to the following general idea. Let us consider two particles Ω_j and Ω_k $(j, k \in \{1, \ldots, N\}\ j \neq k)$. Under the influence of the magnetic field $\mathbf{H_0}$, the particle Ω_j produces an induced magnetic field denoted $\mathbf{H_1}^{(j)}$ and the particle Ω_k produces an induced magnetic field denoted $\mathbf{H_1}^{(k)}$. The non-interacting assumption states that the total magnetic field can be approximated by $\mathbf{H} \approx \mathbf{H_0} + \mathbf{H_1}^{(j)} + \mathbf{H_1}^{(k)}$. Moreover, the effect of the magnetic field $\mathbf{H_1}^{(k)}$ (resp. $\mathbf{H_1}^{(j)}$) on the particle Ω_j (resp. Ω_k) is to produce an induced magnetic field denoted $\mathbf{H_2}^{(j)}$ (resp. $\mathbf{H_2}^{(k)}$). At the first order of approximation, taking into account pairwise magnetic interactions gives rise to the following approximation of the total magnetic field: $\mathbf{H} \approx \mathbf{H_0} + \mathbf{H_1}^{(j)} + \mathbf{H_1}^{(k)} + \mathbf{H_2}^{(j)} + \mathbf{H_2}^{(k)}$. And the process can be continued at higher order of approximation taking into account higher order of mutual interactions: The effect of the magnetic field $\mathbf{H_2}^{(k)}$ (resp. $\mathbf{H_2}^{(j)}$) on the particle Ω_j (resp. Ω_k) is to produce an induced magnetic field denoted $\mathbf{H_3}^{(j)}$ (resp. $\mathbf{H_3}^{(k)}$), etc. Note that since the magnetic field strength decays as the power 3 of the distance to its source, the two particles Ω_j and Ω_k must be very close to each other (nearly touching) so that it is necessary to consider order of approximation higher than one. Besides, the complexity of this approach increases severely with the order of mutual interactions and the number of particles, making it unsuitable for numerical purposes at order higher than one. Thus, in the paper we restrict ourselves to the study of the accuracy of a method based on pairwise magnetic interactions.

Denoting by φ_{c_j,c_k} the magnetic interaction potential of the particle Ω_j located at position c_j on the particle Ω_k located at position c_k, our second main result (Thm. 4.6) states that

$$\Big\|\varphi - \Big(\sum_{j=1}^{N}\varphi_{c_j} + \sum_{j=1}^{N}\sum_{\substack{k=1\\k\neq j}}^{N}\varphi_{c_k,c_j}\Big)\Big\|_{\mathbb{W}^1(\mathbb{R}^3)} \leqslant A_1\,A_4\,(\mu_p-1)\,\lambda_p\,N\,\left(\frac{\varepsilon}{R}\right)^{\frac{3}{2}}\left(\frac{2\varepsilon}{\delta}\right)^{5}$$
$$\times\left(B_3+3\ln\left(\frac{2R}{\delta}\right)\right)\left(B_3\,\mathrm{Li}_{-\frac{3}{2}}\left(\frac{2\varepsilon}{\delta}\right)+3\left(\frac{2\varepsilon}{\delta}\right)\ln\left(\frac{2R}{\delta}\right)\right)R\,|\mathbf{H_0}|,$$

where $A_1A_4 \approx 213$, Li_s denotes to the Polylogarithm function of order s, and $\lambda_p := \frac{(\mu_p-1)^2}{(\mu_p+1)(\mu_p+2)} \in [0,1]$. A $\mathbb{L}^\infty$-bound for the error made by taking into account pairwise interactions is also provided, see Theorem 4.8. By contrast, these sharp estimates provide an insight on the error related to the "non-interacting assumption" with respect to the critical parameters which are: the size of the particles and the minimal distance δ between the particles.

We will not be concerned in the paper with practical aspects of the implementation of the numerical method based on the computation of pairwise magnetic interactions. This point will be the object of a future work.

The paper is organized as follows. In Section 2, we introduce and study the magneto-statics problem. In Section 3, we study the accuracy of the "non-interacting assumption" and prove the above mentioned error estimate together with a point-wise error estimate. In Section 4, we study the approach consisting in taking into account pairwise interactions in the computation of the magnetic potential and we prove the error estimates in that case. Finally, Section 5 is devoted to numerical illustrations.

2. The magnetostatic problem

2.1. Formulation for the scalar magnetic potential

The magnetostatic problem described in introduction, expressed for the magnetic field $\mathbf{H}$, reads

$$\begin{cases} \mathbf{rot}\,\mathbf{H} = \mathbf{0} & \text{in } \mathbb{R}^3 \\ \operatorname{div}\mathbf{H} = 0 & \text{in } \Omega_1,\dots,\Omega_N \text{ and } \Omega^c \\ [\mu\mathbf{H}\cdot\mathbf{n}] = \mathbf{0} & \text{across } \Sigma_1,\dots,\Sigma_N \end{cases} \tag{2.1}$$

where μ is the piecewise constant function taking the value 1 in Ω^c and μ_p in $\Omega_j, j \in \{1,\dots,N\}$. Moreover, we have the following condition at infinity

$$\lim_{\substack{|x|\to+\infty\\x\in\mathbb{R}^3}} \mathbf{H}(x) = \mathbf{H_0} \tag{2.2}$$

where $\mathbf{H_0}$ is the applied magnetic field assumed to be constant in strength and direction. By convenience, we denote by $|\ |$ either the absolute value of a real number or the euclidean norm of a vector in $\mathbb{R}^3$. In (2.1) and throughout the paper, we will denote by $[u]$ the jump of the quantity u across one of the boundaries Σ_j : $[u] = u|_{\Omega^c} - u|_{\Omega_j}$, $j \in \{1,\dots,N\}$. As well, the quantity $\mathbf{n}$ will refer to the outward unit normal to the boundary Σ_j.

We reformulate problem (2.1) in terms of the induced magnetic field $\mathbf{H}'$, such that $\mathbf{H} = \mathbf{H_0} + \mathbf{H}'$. It is natural to assume that $\mathbf{H}'$ belongs to $\mathbb{L}^2(\mathbb{R}^3)^3$ the Hilbert space of square integrable vector functions. Since $\mathbf{H}'$ is curl free, thanks to Poincaré lemma, we can introduce the so-called *scalar magnetic potential* $\varphi \in \mathbb{W}^1_0(\mathbb{R}^3)$ such that

$$\mathbf{H}' = -\nabla\varphi \tag{2.3}$$

where $\mathbb{W}_0^1(\mathbb{R}^3)$ is the weighted Sobolev space defined by

$$\mathbb{W}_0^1(\mathbb{R}^3) = \left\{ \psi \in \mathcal{D}'(\mathbb{R}^3) \ ; \ \frac{\psi}{\sqrt{1+|x|^2}} \in \mathbb{L}^2(\mathbb{R}^3) \ , \nabla\psi \in \mathbb{L}^2(\mathbb{R}^3)^3 \right\}.$$

As outlined in [7] the semi-norm defined by

$$\psi \in \mathbb{W}_0^1(\mathbb{R}^3) \longmapsto \left(\int_{\mathbb{R}^3} |\nabla\psi|^2 \ \mathrm{d}x \right)^{\frac{1}{2}}$$

is a norm on $\mathbb{W}_0^1(\mathbb{R}^3)$, denoted by $\|\cdot\|_{\mathbb{W}^1(\mathbb{R}^3)}$ in the sequel. Moreover, all $\psi \in \mathbb{W}_0^1(\mathbb{R}^3)$ satisfies $[\psi] = 0$ across Σ where Σ denotes any regular surface Σ in $\mathbb{R}^3$. The magnetic potential $\varphi \in \mathbb{W}_0^1(\mathbb{R}^3)$ satisfies the following problem deduced from (2.1)

$$\begin{cases} \Delta\varphi &= 0 & \text{in } \Omega_1, \ldots, \Omega_N \text{ and } \Omega^c \\ \left[\mu \dfrac{\partial\varphi}{\partial n}\right] &= [\mu]\, \mathbf{H_0} \cdot \mathbf{n} & \text{across } \Sigma_1, \ldots \Sigma_N. \end{cases} \tag{2.4}$$

We introduce the following normalization: $x_i = R\,\widetilde{x}_i$ for $i = 1, 2, 3$ where $\widetilde{x}_i$ denotes the dimensionless i-th coordinate. In the dimensionless coordinates system, problem (2.4) for the new unknown $\widetilde{\varphi}$ defined by $|\mathbf{H_0}| R\, \widetilde{\varphi}(\widetilde{x}) = \varphi(R\,\widetilde{x})$ for all $\widetilde{x} \in \mathbb{R}^3$ reads

$$\begin{cases} \Delta\widetilde{\varphi} &= 0 & \text{in } \widetilde{\Omega}_1, \ldots, \widetilde{\Omega}_N \text{ and } \widetilde{\Omega}^c \\ \left[\mu \dfrac{\partial\widetilde{\varphi}}{\partial n}\right] &= [\mu]\, \dfrac{\mathbf{H_0}}{|\mathbf{H_0}|} \cdot \mathbf{n} & \text{across } \widetilde{\Sigma}_1, \ldots, \widetilde{\Sigma}_N \end{cases} \tag{2.5}$$

where $\widetilde{\Omega}_j = B(\widetilde{c}_j, \widetilde{\varepsilon})$, $\widetilde{c}_j = c_j/R$, $\widetilde{\varepsilon} = \varepsilon/R$ and $\widetilde{\Omega}^c = \mathbb{R}^3 \setminus \bigcup_{j=1}^N \overline{\widetilde{\Omega}_j}$. We also set $\widetilde{\delta} = \delta/R$. Note that the conditions (1.2) give rise to the conditions

$$2\widetilde{\varepsilon} < \widetilde{\delta} < \frac{8}{N} < 1. \tag{2.6}$$

From now on, we will only consider the dimensionless problem (2.5) and, for convenience, we will drop the tilde symbol $(\widetilde{\ })$ introduced to distinguish dimensionless quantities. As well, we do not write down vectors in bold letters anymore.

Thus, we have a magnetostatic problem in the form:

$$\begin{cases} \Delta\varphi &= 0 & \text{in } \Omega_1, \ldots, \Omega_N \text{ and } \Omega^c \\ \left[\mu \dfrac{\partial\varphi}{\partial n}\right] &= [\mu]\, h & \text{across } \Sigma_1, \ldots, \Sigma_N \end{cases} \tag{2.7}$$

for a given $h \in \mathbb{L}^\infty(\Sigma)$. The weak formulation of problem (2.7) reads: find $\varphi \in \mathbb{W}_0^1(\mathbb{R}^3)$ such that for all $\psi \in \mathbb{W}_0^1(\mathbb{R}^3)$

$$\int_{\Omega^c} \nabla\varphi \cdot \nabla\psi \ \mathrm{d}x + \mu_p \sum_{j=1}^N \int_{\Omega_j} \nabla\varphi \cdot \nabla\psi \ \mathrm{d}x = (\mu_p - 1) \sum_{j=1}^N \oint_{\Sigma_j} h\,\psi \ \mathrm{d}\sigma. \tag{2.8}$$

A direct application of Lax–Milgram theorem proves that problem (2.8) has a unique solution $\varphi \in \mathbb{W}_0^1(\mathbb{R}^3)$. Moreover, using φ as a test function in (2.8), we get

$$\|\varphi\|^2_{\mathbb{W}^1(\mathbb{R}^3)} \leqslant (\mu_p - 1) \sum_{j=1}^N \|h\|_{\mathbb{L}^\infty(\Sigma_j)} \|\varphi\|_{\mathbb{L}^1(\Sigma_j)} \tag{2.9}$$

and from the trace inequality (A.1) given on Appendix A, we deduce that

$$\|\varphi\|_{\mathbb{W}^1(\mathbb{R}^3)} \leqslant A_1\,(\mu_p-1)\,N\,\varepsilon^{\frac{3}{2}}\,\|h\|_{\mathbb{L}^\infty(\Sigma)}, \tag{2.10}$$

where $\|h\|_{\mathbb{L}^\infty(\Sigma)} = \sup_{j\in\{1,\dots,N\}}\|h\|_{\mathbb{L}^\infty(\Sigma_j)}$ and where $A_1 = \sqrt{4\pi}$. Applying these results in the special case when $h = \frac{H_0}{|H_0|}\cdot n$ whose $\mathbb{L}^\infty$-norm equals 1, we have proven the following proposition.

Proposition 2.1. *There exists a unique $\varphi \in \mathbb{W}^1_0(\mathbb{R}^3)$ solution to problem (2.5). It satisfies*

$$\|\varphi\|_{\mathbb{W}^1(\mathbb{R}^3)} \leqslant A_1\,(\mu_p-1)\,N\,\varepsilon^{\frac{3}{2}}, \tag{2.11}$$

where $A_1 = \sqrt{4\pi}$.

2.2. The one particle case as a reference problem

We consider the following reference problem: find $\varphi_{\text{ref}} \in \mathbb{W}^1_0(\mathbb{R}^3)$ such that

$$\begin{cases} \Delta\varphi_{\text{ref}} &= 0 \qquad \text{in } B(0,\varepsilon) \text{ and } \complement\overline{B}(0,\varepsilon) \\ \left[\mu\dfrac{\partial\varphi_{\text{ref}}}{\partial n}\right] &= [\mu]\,h \qquad \text{across } S(0,\varepsilon) = \partial B(0,\varepsilon) \end{cases} \tag{2.12}$$

where $\complement\overline{B}(0,\varepsilon)$ denotes the complement of the adherence of the ball $B(0,\varepsilon)$, $\mu = \mu_p$ in $B(0,\varepsilon)$, $\mu = 1$ in $\complement\overline{B}(0,\varepsilon)$ and $h = \frac{H_0}{|H_0|}\cdot n$. For convenience, we consider a reference frame $(0, e_1, e_2, e_3)$ such that H_0 defines the direction of e_3. With this convention, we have $h = e_3\cdot n$. Problem (2.12) admits a unique solution $\varphi_{\text{ref}} \in \mathbb{W}^1_0(\mathbb{R}^3)$. (Indeed, it corresponds to problem (2.7) in the special case when $N = 1$ and $\Omega_1 = B(0,\varepsilon)$.) In this simple geometrical framework, the solution φ_{ref} can be computed analytically using the separation of variables method in spherical coordinates. We obtain

$$\varphi_{\text{ref}}(x) = \begin{cases} \dfrac{\mu_p-1}{\mu_p+2}\; e_3\cdot x & \text{in } B(0,\varepsilon) \\ \dfrac{\mu_p-1}{\mu_p+2}\;\dfrac{\varepsilon^3}{|x|^3}\; e_3\cdot x & \text{in } \complement\overline{B}(0,\varepsilon). \end{cases} \tag{2.13}$$

Moreover, the gradient of φ_{ref} is given by

$$\nabla\varphi_{\text{ref}}(x) = \begin{cases} -\dfrac{\mu_p-1}{\mu_p+2}\; e_3 & \text{in } B(0,\varepsilon) \\ -\dfrac{\mu_p-1}{\mu_p+2}\;\dfrac{\varepsilon^3}{|x|^3}\left(3\big(e_3\cdot x\big)\,\dfrac{x}{|x|^2} - e_3\right) & \text{in } \complement\overline{B}(0,\varepsilon). \end{cases} \tag{2.14}$$

From (2.13) and (2.14) we deduce the following estimates.

Proposition 2.2. *Let φ_{ref} be the solution to problem (2.12). For all $x \in \complement\overline{B}(0,\varepsilon)$, we have*

$$|\varphi_{\text{ref}}(x)| \leqslant \frac{\mu_p-1}{\mu_p+2}\,\frac{\varepsilon^3}{|x|^2} \qquad \text{and} \qquad |\nabla\varphi_{\text{ref}}(x)| \leqslant 2\,\frac{\mu_p-1}{\mu_p+2}\,\frac{\varepsilon^3}{|x|^3}. \tag{2.15}$$

For a spherical particle with radius ε centered at position $c_j \in \mathbb{R}^3$, introducing the translation mapping

$$T_{c_j} : x \in \mathbb{R}^3 \longmapsto x - c_j \in \mathbb{R}^3, \tag{2.16}$$

we readily obtain that the function $\varphi_{c_j} = \varphi_{\text{ref}}\circ T_{c_j}$ satisfies

$$\begin{cases} \Delta\varphi_{c_j} &= 0 \qquad \text{in } \;\Omega_j \text{ and } \complement\overline{\Omega}_j \\ \left[\mu\dfrac{\partial\varphi_{c_j}}{\partial n}\right] &= [\mu]\,h \qquad \text{across } \;\Sigma_j\;. \end{cases} \tag{2.17}$$

The situation is illustrated in Figure 2. The solution φ_{c_j} to problem (2.17) is the magnetic potential induced by the metallic particle Ω_j submitted to the magnetic field H_0.

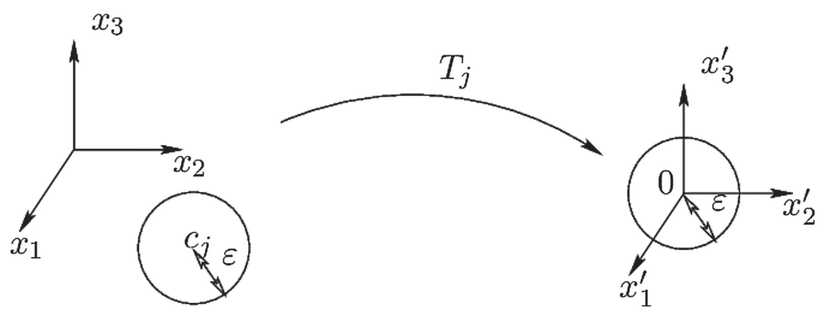

FIGURE 2. Notations for the translation of the coordinates system.

3. Accuracy of the non-interaction assumption

3.1. Approximation under the non-interacting assumption

The solution φ to problem (2.5) can be expressed as

$$\varphi = \sum_{j=1}^{N} \varphi_{c_j} + \psi. \tag{3.1}$$

The sum can be interpreted as the scalar magnetic potential induced by the metallic particles under the assumption that they do not interact together. Since outside a particle, the magnetic field induced by the particle decreases as $1/r^3$ where r denotes the distance to the particle center (see Prop. 2.2), if the particles are at a distance sufficiently large from each other, or if the solid fraction of particles is small, their mutual interaction contribution to the total induced magnetic field can be neglected and it would be reasonable to expect that the approximation $\varphi \approx \sum_{j=1}^{N} \varphi_{c_j}$ is of good quality. However, if the particles are "not too far" from each other, or if the volume solid fraction of particles is "not too small", this approximation is not anymore accurate. We want to quantify what "not too far" or "not to small" means by studying the behavior of the correction term ψ.

Proposition 3.1. *The function ψ introduced in (3.1) belongs to $\mathbb{W}_0^1(\mathbb{R}^3)$ and satisfies*

$$\begin{cases} \Delta\psi & = 0 \qquad \text{in } \Omega_1, \dots, \Omega_N \text{ and } \Omega^c \\ \left[\mu \dfrac{\partial \psi}{\partial n}\right] & = [\mu]\, g_0 \qquad \text{across } \Sigma_1, \dots, \Sigma_N \end{cases} \tag{3.2}$$

where the data g_0 is defined for all $x \in \Sigma_i$, $i \in \{1, \dots, N\}$, by

$$g_0(x) = -\sum_{\substack{j=1 \\ j \neq i}}^{N} \nabla\varphi_{\mathrm{ref}}(T_{c_j}(x)) \cdot n(x). \tag{3.3}$$

Proof. By linearity, ψ belongs to $\mathbb{W}_0^1(\mathbb{R}^3)$ and satisfies the Laplace equation in each domain $\Omega_i, i \in \{1, \dots, N\}$ and in Ω^c, together with the following interface conditions across $\Sigma_i, i \in \{1, \dots, N\}$:

$$\left[\mu \frac{\partial \psi}{\partial n}\right] = \left[\mu \frac{\partial \varphi}{\partial n}\right] - \sum_{j=1}^{N} \left[\mu \frac{\partial \varphi_{c_j}}{\partial n}\right] \cdot \tag{3.4}$$

Let $i \in \{1, \dots, N\}$. From (2.5) and (2.17), we have the following condition at the interface Σ_i

$$\left[\mu \frac{\partial \varphi}{\partial n}\right] = [\mu]\, h \quad \text{and} \quad \left[\mu \frac{\partial \varphi_{c_i}}{\partial n}\right] = [\mu]\, h.$$

We deduce that

$$\left[\mu\frac{\partial\psi}{\partial n}\right] = -\sum_{\substack{j=1\\ j\neq i}}^{N}\left[\mu\frac{\partial\varphi_{c_j}}{\partial n}\right] \qquad \text{across } \Sigma_i. \tag{3.5}$$

For any $j \in \{1,\dots,N\}$, $j \neq i$, the potential φ_{c_j} solution to problem (2.17) is continuous in $\mathbb{R}^3$ and it is regular (regularity $\mathcal{C}^\infty$) everywhere except on the boundary Σ_j. Since for all $j \neq i$ we have $|c_i - c_j| > 2\varepsilon$ (this condition states that the particles Ω_i and Ω_j with radius ε do not intersect), the normal derivative $\frac{\partial\varphi_{c_j}}{\partial n}$ is continuous across Σ_i so that (3.5) also reads

$$\left[\mu\frac{\partial\psi}{\partial n}\right] = -[\mu]\sum_{\substack{j=1\\ j\neq i}}^{N}\frac{\partial\varphi_{c_j}}{\partial n} = -[\mu]\left(\sum_{\substack{j=1\\ j\neq i}}^{N}\nabla\varphi_{\mathrm{ref}}\circ T_{c_j}\right)\cdot n_{|\Sigma_i}. \tag{3.6}$$

Proposition 3.1 is proved. □

3.2. $\mathbb{W}^1$-estimate of the error under the non-interacting assumption

Proposition 3.2. *The source term g_0 defined in (3.3) is such that*

$$\|g_0\|_{\mathbb{L}^\infty(\Sigma)} \leqslant 2\frac{\mu_p - 1}{\mu_p + 2}\left(\frac{2\varepsilon}{\delta}\right)^3\left(B_3 + 3\ln\left(\frac{2}{\delta}\right)\right) \tag{3.7}$$

where $B_3 = 142 + 3\ln 2 \approx 144.1$.

Proof. The proof relies on Proposition 2.2. For all $x \in \Sigma_i$, we have

$$|g_0(x)| \leqslant \sum_{\substack{j=1\\ j\neq i}}^{N}\left|\nabla\varphi_{\mathrm{ref}}(T_{c_j}(x))\right| \leqslant 2\frac{\mu_p-1}{\mu_p+2}\sum_{\substack{j=1\\ j\neq i}}^{N}\frac{\varepsilon^3}{|T_{c_j}(x)|^3}. \tag{3.8}$$

The quantity $\left|T_{c_j}(x)\right|$ is the distance from the center c_j of the particle Ω_j to the point $x \in \Sigma_i$, see Figure 3. It is shown in Appendix B, see relation (B.1), that

$$\sum_{\substack{j=1\\ j\neq i}}^{N}\frac{1}{|T_{c_j}(x)|^3} \leqslant \left(B_3 + 3\ln\left(\frac{2}{\delta}\right)\right)\left(\frac{2}{\delta}\right)^3. \tag{3.9}$$

Combining (3.8) and (3.9) gives the estimate. □

Note that problem (3.2) for ψ has the form of problem (2.7) for φ for the boundary data $h = g_0$. As a direct consequence of (2.10) and (3.7), we have the following result.

Theorem 3.3. *Let $\Omega_1,\dots,\Omega_N$ be N spherical particles in $B(0,1) \subset \mathbb{R}^3$, centered respectively at c_j, $j \in \{1,\dots,N\}$, with the same radius $\varepsilon > 0$. Let δ be the minimal distance between two particles as defined in (1.1). Let $\varphi_{c_j} = \varphi_{\mathrm{ref}}\circ T_{c_j}$ where φ_{ref} is given by (2.13) be the magnetic potential induced by particle Ω_j taken in isolation from the others. We have*

$$\left\|\varphi - \sum_{j=1}^{N}\varphi_{c_j}\right\|_{\mathbb{W}^1(\mathbb{R}^3)} \leqslant 2A_1\frac{(\mu_p-1)^2}{\mu_p+2}N\,\varepsilon^{\frac{3}{2}}\left(\frac{2\varepsilon}{\delta}\right)^3\left(B_3 + 3\ln\left(\frac{2}{\delta}\right)\right) \tag{3.10}$$

where $A_1 = \sqrt{4\pi}$ and $B_3 = 142 + 3\ln 2 \approx 144.1$.

Remark 3.4. In terms of our key parameters, the bound given in relation (3.10) for the first order error term in our asymptotic expansion of the magnetic potential φ is the product of $N\varepsilon^{\frac{3}{2}}$ (which is the order of φ, see estimate (2.11)), by a complementary term comparable to $\left(\frac{2\varepsilon}{\delta}\right)^3\left(1 + \ln\left(\frac{2}{\delta}\right)\right)$.

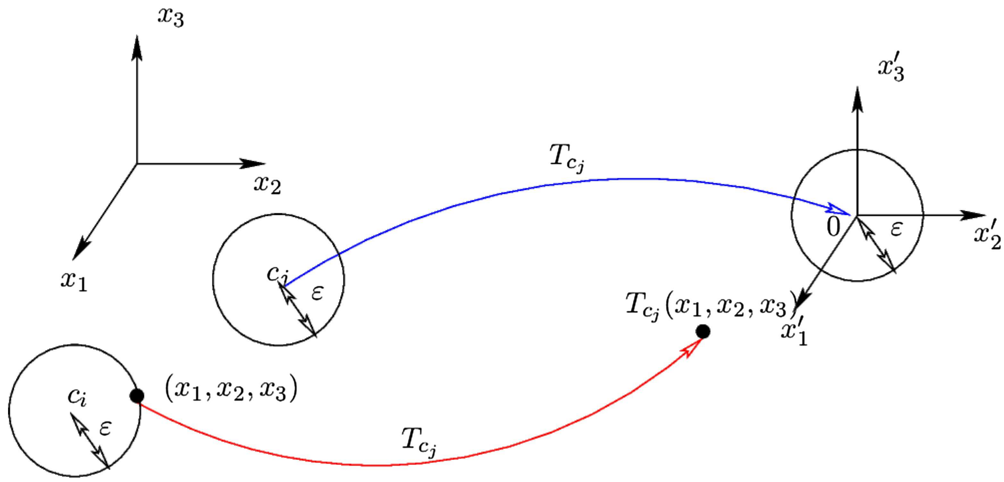

FIGURE 3. Effect of the translation of the coordinates system for several particles.

3.3. $\mathbb{L}^\infty$-estimate of the error under the non-interacting assumption

Now, we are interested in providing a point-wise estimate for $\psi = \varphi - \sum_{j=1}^N \varphi_{c_j}$. While the estimate of $\|\psi\|_{\mathbb{W}^1(\mathbb{R}^3)}$ was based on Lax–Milgram theorem, our point-wise estimate for ψ relies on integral representation formula for the Laplacian. Namely, the solution ψ to (3.2) can be expressed, for all $x \in \Omega^c$, as ([6], Thm 2, p. 120)

$$\psi(x) = -(\mu_p - 1) \sum_{j=1}^N \left(\int_{\Sigma_j} g_0(y)\, \mathcal{G}(x, y)\ \mathrm{d}y - \int_{\Sigma_j} \psi(y)\, \partial_n \mathcal{G}(x, y)\ \mathrm{d}y \right) \tag{3.11}$$

where $\mathcal{G}$, the Green kernel of the Laplacian in $\mathbb{R}^3$, and its normal derivative on Σ_j, denoted $\partial_n \mathcal{G}$, are given by:

$$\mathcal{G}(x, y) = \frac{1}{4\pi |x - y|}, \qquad \partial_n \mathcal{G}(x, y) = \frac{n \cdot (x - y)}{4\pi |x - y|^3}. \tag{3.12}$$

We deduce from (3.11), the following estimate for ψ:

$$|\psi(x)| \leqslant (\mu_p - 1) \sum_{j=1}^N \left(\|g_0\|_{\mathbb{L}^\infty(\Sigma_j)}\, \|\mathcal{G}(x, \cdot)\|_{\mathbb{L}^1(\Sigma_j)} + \|\psi\|_{\mathbb{L}^4(\Sigma_j)}\, \|\partial_n \mathcal{G}(x, \cdot)\|_{\mathbb{L}^{\frac{4}{3}}(\Sigma_j)} \right) \tag{3.13}$$

where the choice of the norms involved in (3.13) are guided by the regularity of Green's kernel. Indeed, it is known (see [6], Rem. 4, p. 127), that $\mathcal{G}(x, \cdot)$ is integrable on any boundary Σ_j and that $\partial_n \mathcal{G}(x, \cdot)$ belongs to $\mathbb{L}^p(\Sigma_j)$ for all $p < 2$. Having a $\mathbb{L}^\infty(\Sigma_j)$ estimate on g_0 (see Prop. 3.1), the way the first integral is bounded is a natural choice. Concerning the second integral, we will use the fact that the Sobolev and trace inequalities imply that $\|\psi\|_{\mathbb{L}^4(\Sigma_j)} \leqslant A_2 \|\psi\|_{\mathbb{W}^1(\mathbb{R}^3)}$ where $A_2 = 2/(3^{\frac{3}{8}} \sqrt{\pi})$ (see Prop. A.2), and that ψ is controlled in $\mathbb{W}^1(\mathbb{R}^3)$-norm (see Thm. 3.3). Our point-wise estimate for ψ relies on the estimates provided in the following lemma.

Lemma 3.5. *Let $\Omega_1, \ldots, \Omega_N$ be N isolated spherical particles in $B(0, 1) \subset \mathbb{R}^3$, with boundaries $\Sigma_1, \ldots, \Sigma_N$, respectively centered at $c_1, \ldots, c_N$ with the same radius ε. Let δ be the minimal distance between two particles as defined in* (1.1)*. For all $x \in \mathbb{R}^3$, we have*

$$\sum_{j=1}^N \|\mathcal{G}(x, \cdot)\|_{\mathbb{L}^1(\Sigma_j)} \leqslant B_1 \left(\frac{2}{\delta} \right)^3 \varepsilon^2 + M_x\, \varepsilon \tag{3.14a}$$

$$\text{and} \qquad \sum_{j=1}^{N} \|\partial_n \mathcal{G}(x,\cdot)\|_{\mathbb{L}^{\frac{4}{3}}(\Sigma_j)} \leqslant B_2 \left(\frac{2}{\delta}\right)^3 \varepsilon^{\frac{3}{2}} + M_x\, A_3\, \varepsilon^{\frac{3}{2}} \tag{3.14b}$$

where $M_x \leqslant \min(64, N)$ corresponds to the number of particles whose distance at x is less than 2δ and the other constants are such that $B_1 \approx 8.385$, $B_2 \approx 6.611$ and $A_3 \approx 0.3439$ (all the constants introduced throughout the paper are summarized in Tab. E.1, p. 1108).

Proof. Let us start by proving the estimate for $\mathcal{S}_1 := \sum_{j=1}^{N} \|\mathcal{G}(x,\cdot)\|_{\mathbb{L}^1(\Sigma_j)}$. For $x \in \Omega^c$ and for $j \in \{1,\dots,N\}$, the quantity $\|\mathcal{G}(x,\cdot)\|_{\mathbb{L}^1(\Sigma_j)}$ is the solution to the following problem (see [6], Thm. 2, p. 120):

$$\begin{cases} \Delta u = 0 & \text{in } \ \Omega_j \text{ and } \mathbb{R}^3 \setminus \overline{\Omega_j} \\ [u] = 0 & \text{across } \ \Sigma_j \\ [\partial_n u] = 1 & \text{across } \ \Sigma_j. \end{cases} \tag{3.15}$$

The solution to problem (3.15) can be computed analytically by using the separation of variables method in spherical coordinates. It is found to be:

$$u = \|\mathcal{G}(x,\cdot)\|_{\mathbb{L}^1(\Sigma_j)} = \begin{cases} \dfrac{\varepsilon^2}{|x-c_j|} & \text{if } x \in \mathbb{R}^3 \setminus \overline{\Omega_j} \\ \varepsilon & \text{if } x \in \overline{\Omega_j}. \end{cases} \tag{3.16}$$

We split the sum $\mathcal{S}_1$ into two parts. The first one, denoted $\mathcal{S}_1^{\text{near}}$ in the sequel, corresponds to the indexes j such that the center c_j of the particle Ω_j is at a distance of x smaller than 2δ and the second one, denoted $\mathcal{S}_1^{\text{far}}$ in the sequel, corresponds to the indexes j such that the center c_j is at a distance of x strictly larger than 2δ. Accordingly,

$$\mathcal{S}_1 = \sum_{\substack{i=1 \\ |x-c_i|<2\delta}}^{N} \|\mathcal{G}(x,\cdot)\|_{\mathbb{L}^1(\Sigma_i)} + \sum_{\substack{j=1 \\ |x-c_j|\geqslant 2\delta}}^{N} \|\mathcal{G}(x,\cdot)\|_{\mathbb{L}^1(\Sigma_j)} := \mathcal{S}_1^{\text{near}} + \mathcal{S}_1^{\text{far}}. \tag{3.17}$$

The number M_x of terms in the sum $\mathcal{S}_1^{\text{near}}$ is bounded independently of N. Since $x \in \Omega^c$, M_x corresponds to the number of disjointed balls of radius 1 that can be contained in a ball of radius 4. By volume consideration, one can show that $M_x \leqslant 64$. From (3.16), we deduce that $\mathcal{S}_1^{\text{near}} \leqslant M_x\, \varepsilon$.

Using relation (3.16) and a strategy similar to the one used in Appendix B to show relations (B.1) and (B.2), we have

$$\begin{aligned} \mathcal{S}_1^{\text{far}} &= \sum_{\substack{j=1 \\ |x-c_j|\geqslant 2\delta}}^{N} \frac{\varepsilon^2}{|x-c_j|} = \frac{6\,\varepsilon^2}{\pi\delta^3} \sum_{\substack{j=1 \\ |x-c_j|\geqslant 2\delta}}^{N} \int_{B(c_j,\frac{\delta}{2})} \frac{\mathrm{d}y}{|x-c_j|} \\ &\leqslant \frac{6\,\varepsilon^2}{\pi\delta^3} \sum_{\substack{j=1 \\ |x-c_j|\geqslant 2\delta}}^{N} \int_{B(c_j,\frac{\delta}{2})} \frac{\mathrm{d}y}{|x-y|-\frac{\delta}{2}} \leqslant \frac{6\,\varepsilon^2}{\pi\delta^3} \int_{B(x,2+\frac{\delta}{2})\setminus B(x,\frac{3\delta}{2})} \frac{\mathrm{d}y}{|x-y|-\frac{\delta}{2}} \\ &\leqslant \frac{24\,\varepsilon^2}{\delta^3} \int_{\frac{3\delta}{2}}^{2+\frac{\delta}{2}} \frac{r^2\,\mathrm{d}r}{r-\frac{\delta}{2}} = \frac{24\,\varepsilon^2}{\delta^3} \int_{\delta}^{2} \frac{(s+\frac{\delta}{2})^2\,\mathrm{d}s}{s} \leqslant B_1 \left(\frac{2}{\delta}\right)^3 \varepsilon^2 \end{aligned}$$

where we have introduced the constant

$$B_1 = \max_{\delta>0} \int_{\delta}^{2} \frac{3(s+\frac{\delta}{2})^2\,\mathrm{d}s}{s} = 3 \max_{\delta>0} \left(2 + 2\delta - \frac{3\delta^2}{2} + \frac{\delta^2}{4} \ln\left(\frac{2}{\delta}\right)\right) \approx 8.385.$$

We finally deduce that

$$\mathcal{S}_1 = \mathcal{S}_1^{\text{near}} + \mathcal{S}_1^{\text{far}} \leqslant B_1 \left(\frac{2}{\delta}\right)^3 \varepsilon^2 + M_x\, \varepsilon \tag{3.18}$$

where the contribution $M_x\,\varepsilon$ is actually only present if x is at a distance less than 2δ from at least one particle.

The estimate for $\mathcal{S}_2 := \sum_{j=1}^N \|\partial_n \mathcal{G}(x,\cdot)\|_{\mathbb{L}^{\frac{4}{3}}(\Sigma_j)}$ is obtained in a very similar way. We split the sum over j into two parts $\mathcal{S}_2^{\text{near}}$ and $\mathcal{S}_2^{\text{far}}$ according to the distance between the point x and the spheres Σ_j:

$$\mathcal{S}_2 = \sum_{\substack{i=1\\|x-c_i|\leqslant 2\delta}}^N \|\partial_n \mathcal{G}(x,\cdot)\|_{\mathbb{L}^{\frac{4}{3}}(\Sigma_i)} + \sum_{\substack{j=1\\|x-c_j|>2\delta}}^N \|\partial_n \mathcal{G}(x,\cdot)\|_{\mathbb{L}^{\frac{4}{3}}(\Sigma_j)} := \mathcal{S}_2^{\text{near}} + \mathcal{S}_2^{\text{far}}. \tag{3.19}$$

The number of terms in the first sum $\mathcal{S}_2^{\text{near}}$ is, as before, bounded by M_x, independently of N. In order to estimate the quantity $\|\partial_n \mathcal{G}(x,\cdot)\|_{\mathbb{L}^{\frac{4}{3}}(\Sigma_i)}$ when $|x-c_i|<2\delta$, we first introduce the projection $x^\star$ of x on Σ_i. We note that (see Appendix D)

$$\forall y\in\Sigma_i \qquad |\partial_n \mathcal{G}(x,y)| \leqslant |\partial_n \mathcal{G}(x^\star,y)|$$

and that the quantity $\|\partial_n \mathcal{G}(x^\star,\cdot)\|_{\mathbb{L}^{\frac{4}{3}}(\Sigma_i)}$ can be explicitly evaluated (see Appendix D for details). We have

$$\|\partial_n \mathcal{G}(x,\cdot)\|_{\mathbb{L}^{\frac{4}{3}}(\Sigma_i)} \leqslant A_3\,\varepsilon^{\frac{3}{2}} \tag{3.20}$$

where $A_3 = \|\partial_n \mathcal{G}((1,0,0),\cdot)\|_{\mathbb{L}^{\frac{4}{3}}(S^2)} \approx 0.3439$. (The result is proven in Appendix D for a ball of radius 1 but by dilation one easily reveals the factor $\varepsilon^{\frac{3}{2}}$). Finally, we obtain

$$\mathcal{S}_2^{\text{near}} \leqslant M_x\,A_3\,\varepsilon^{\frac{3}{2}}.$$

Let us now consider the sum $\mathcal{S}_2^{\text{far}}$ in (3.19) over the indexes j such that x is at a distance larger than 2δ from the center c_j of the particle Ω_j. For x such that $|x-c_i|>2\delta$ and for $y\in\Sigma_j$, we have

$$|x-y| \geqslant |x-c_i| - \varepsilon \geqslant \frac{2\delta-\varepsilon}{2\delta}|x-c_j| > \frac{3}{4}|x-c_j|$$

so that

$$\|\partial_n \mathcal{G}(x,\cdot)\|_{\mathbb{L}^{\frac{4}{3}}(\Sigma_j)} \leqslant \frac{1}{4\pi}\left(\oint_{\Sigma_j}\frac{\mathrm{d}y}{|x-y|^{\frac{8}{3}}}\right)^{\frac{3}{4}} \leqslant \frac{4}{9\pi}\left(\oint_{\Sigma_j}\frac{\mathrm{d}y}{|x-c_j|^{\frac{8}{3}}}\right)^{\frac{3}{4}} = \frac{4}{9\pi}(4\pi\varepsilon^2)^{\frac{3}{4}}\frac{1}{|x-c_j|^2}. \tag{3.21}$$

Summing over j and using the same strategy as in the case of the sum $\mathcal{S}_1^{\text{far}}$, we deduce that

$$\mathcal{S}_2^{\text{far}} \leqslant B_2\left(\frac{2}{\delta}\right)^3 \varepsilon^{\frac{3}{2}}$$

where $B_2 = \frac{\sqrt{2}}{3\,\pi^{\frac{1}{4}}}\max_{\delta>0}\left(8-6\delta-\delta^2+8\delta\ln(\frac{2}{\delta})\right) \approx 6.611$. We finally deduce that

$$\mathcal{S}_2 = \mathcal{S}_2^{\text{near}} + \mathcal{S}_2^{\text{far}} \leqslant B_2\left(\frac{2}{\delta}\right)^3 \varepsilon^{\frac{3}{2}} + M_x\,A_3\,\varepsilon^{\frac{3}{2}}$$

where the contribution $M_x\,A_3\,\varepsilon^{\frac{3}{2}}$ is only present if x is at a distance smaller than 2δ to any ball. $\square$

We are now in position to state the following point-wise estimate for ψ under the same assumptions as for Theorem 3.3.

Theorem 3.6. *Let $\Omega_1, \ldots, \Omega_N$ be N isolated spherical particles in $B(0,1) \subset \mathbb{R}^3$, centered respectively at c_j, $j \in \{1, \ldots, N\}$, with the same radius ε. Let δ be the minimal distance between two particles as defined in (1.1). Let $\varphi_{c_j} = \varphi_{\text{ref}} \circ T_{c_j}$, where φ_{ref} is given by (2.13), be the magnetic potential induced by the particle Ω_j taken in isolation from the others. For all $x \in \Omega^c$, we have*

$$\Big|\varphi(x) - \sum_{j=1}^{N} \varphi_{c_j}(x)\Big| \leqslant 2\frac{(\mu_p - 1)^2}{\mu_p + 2}\left(\frac{2\varepsilon}{\delta}\right)^3 \varepsilon \left(B_3 + 3\ln\left(\frac{2}{\delta}\right)\right)\left(B_1\left(\frac{2}{\delta}\right)^3 \varepsilon + M_x \right.$$
$$\left. + A_1 A_2\,(\mu_p - 1)\,N\,\varepsilon^2\Big(B_2\left(\frac{2}{\delta}\right)^3 + M_x\,A_3\Big)\right) \tag{3.22}$$

where $M_x \leqslant \min(64, N)$ corresponds to the number of particles whose distance at x is less than 2δ and $A_1, A_2, , A_3, B_1, B_2$ are positive constants (see Tab. E.1, p. 1108 for their full expressions and values).

Proof. From (3.13), $\psi = \varphi - \sum_{j=1}^{N} \varphi_{c_j}$ satisfies for all $x \in \Omega^c$,

$$|\psi(x)| \leqslant (\mu_p - 1)\sum_{j=1}^{N}\Big(\|g_0\|_{\mathbb{L}^\infty(\Sigma_j)}\,\|\mathcal{G}(x,\cdot)\|_{\mathbb{L}^1(\Sigma_j)} + \|\psi\|_{\mathbb{L}^4(\Sigma_j)}\,\|\partial_n \mathcal{G}(x,\cdot)\|_{\mathbb{L}^{\frac{4}{3}}(\Sigma_j)}\Big). \tag{3.23}$$

From Lemma 3.5, we have the estimates

$$\sum_{j=1}^{N} \|\mathcal{G}(x,\cdot)\|_{\mathbb{L}^1(\Sigma_j)} \leqslant B_1\left(\frac{2}{\delta}\right)^3 \varepsilon^2 + M_x\,\varepsilon$$
$$\sum_{j=1}^{N} \|\partial_n \mathcal{G}(x,\cdot)\|_{\mathbb{L}^{\frac{4}{3}}(\Sigma_j)} \leqslant B_2\left(\frac{2}{\delta}\right)^3 \varepsilon^{\frac{3}{2}} + M_x\,A_3\,\varepsilon^{\frac{3}{2}}$$

and $\|g_0\|_{\mathbb{L}^\infty(\Sigma_j)}$ is estimated in Proposition 3.2 so that it remains to estimate $\|\psi\|_{\mathbb{L}^4(\Sigma_j)}$. From the trace theory and Sobolev embedding results, we deduce (see Appendix A for details):

$$\forall\, j \in \{1, \ldots, N\} \qquad \|\psi\|_{\mathbb{L}^4(\Sigma_j)} \leqslant A_2 \|\psi\|_{\mathbb{W}^1(\mathbb{R}^3)}, \tag{3.24}$$

where $A_2 = \frac{2}{3^{\frac{3}{8}}\sqrt{\pi}}$. Since ψ is solution to problem (3.2) which differs from problem (2.7) only by the boundary data h, ψ satisfies the estimate (2.10) with h replaced by g_0, *i.e.* for all $j \in \{1, \ldots, N\}$, we have

$$\|\psi\|_{L^4(\Sigma_j)} \leqslant A_1 A_2\,(\mu_p - 1)\,N\,\varepsilon^{\frac{3}{2}}\,\|g_0\|_{\mathbb{L}^\infty(\Sigma)}. \tag{3.25}$$

□

Remark 3.7. Both Theorems 3.3 and 3.6 can be interpreted as follows. In the extreme case when we consider only two particles, the error made by adding the contribution of the two particles to the magnetic potential assuming no mutual influence is roughly speaking proportional to the cube of the ratio of the particles radius to the distance separating the two particles. In the other extreme case when considering a very large number of particles able to fill the area of interest completely and evenly, the ratio $\frac{\varepsilon^3}{\delta^3}$ is proportional to the volume fraction of particles. Thus, when the volume fraction is low, that is to say when the particles are spaced at a fairly large distance from each other, computing the magnetic potential by neglecting magnetic field reciprocal interactions between particles gives a quite accurate approximation.

4. Taking into account pairwise interactions

4.1. Reference problem for pairwise interactions

When the approximation $\varphi \approx \sum_{j=1}^{N} \varphi_{c_j}$ is not accurate enough, one can compute the error term ψ in (3.1) using the same idea as the one introduced in the previous section for the magnetic potential φ, that is to say by expanding ψ as

$$\psi = \sum_{j=1}^{N} \sum_{\substack{k=1 \\ k \neq j}}^{N} \varphi_{c_k,c_j} + \chi \tag{4.1}$$

where φ_{c_k,c_j}, $j,k \in \{1,\dots,N\}$, $k \neq j$, are found to satisfiy

$$\begin{cases} \Delta \varphi_{c_k,c_j} &= 0 & \text{in } \Omega_j \text{ and } \complement\overline{\Omega}_j \\ \left[\mu \dfrac{\partial \varphi_{c_k,c_j}}{\partial n}\right] &= [\mu]\,(\nabla \varphi_{\mathrm{ref}} \circ T_{c_k}) \cdot n & \text{across } \Sigma_j. \end{cases} \tag{4.2}$$

The gradient of φ_{c_k,c_j} is the magnetic field, denoted $H_2^{(j)}$ in the introduction, induced by the particle Ω_j subjected to the magnetic field $H_1^{(k)}$ where $H_1^{(k)} = \nabla\varphi_{\mathrm{ref}} \circ T_{c_k}$ is the magnetic field induced by the particle Ω_k subjected to the magnetic field H_0.

It should be noted that each couple of functions $(\varphi_{c_j,c_k}, \varphi_{c_k,c_j})$ is related to the potential created by the two particles Ω_j and Ω_k. Namely, the sum $\varphi_{c_j} + \varphi_{c_k} + \varphi_{c_j,c_k} + \varphi_{c_k,c_j}$ corresponds to the potential created by the two particles Ω_j and Ω_k, without taking into account the other particles. Note also that $\varphi_{c_j,c_k} \neq \varphi_{c_k,c_j}$.

The solution φ_{c_k,c_j} to problem (4.2) can be expressed as

$$\varphi_{c_k,c_j} = \varphi_{c_k - c_j,0} \circ T_{c_j} \tag{4.3}$$

where $\varphi_{c_k-c_j,0} \in \mathbb{W}_0^1(\mathbb{R}^3)$ is solution to the following reference problem for $u = c_k - c_j$

$$\begin{cases} \Delta \psi_{\mathrm{ref}}^u &= 0 & \text{in } B(0,\varepsilon) \text{ and } \complement\overline{B}(0,\varepsilon) \\ \left[\mu \dfrac{\partial \psi_{\mathrm{ref}}^u}{\partial n}\right] &= -\,[\mu]\, g^u & \text{across } S(0,\varepsilon) \end{cases} \tag{4.4}$$

where $g^u = -(\nabla\varphi_{\mathrm{ref}} \circ T_u) \cdot n$.

Note that when studying the non-interaction assumption in the last section, the reference problem was independent of the ball center: for symmetry reasons, by a translation one could consider a ball centered at origin. When considering pairwise interactions, there is no more symmetry and the reference problem depends on the relative position of the two balls.

The objective now is to obtain estimates for ψ_{ref}^u similar to the ones obtained for φ_{ref} in Proposition 2.2. The main difficulties are that we do not have an explicit expression for ψ_{ref}^u as it was the case for φ_{ref} and that there is no longer invariance by rotation of the solution to problem (4.4) as it was the case for problem (2.12).

4.2. Explicit solution to the second reference problems

Since ψ_{ref}^u satisfies the Laplace equation, it can be expanded in spherical coordinates (r,θ,η) as

$$\psi_{\mathrm{ref}}^u(r,\theta,\eta) = \sum_{\ell=0}^{+\infty} \sum_{m=-\ell}^{\ell} \left(\alpha_\ell^m\, r^\ell + \beta_\ell^m\, \frac{1}{r^{\ell+1}}\right)\, Y_\ell^m(\theta,\eta) \tag{4.5}$$

where α_ℓ^m and β_ℓ^m are complex numbers to be determined and Y_ℓ^m denotes the Spherical Surface Harmonic function of degree ℓ and order m [25].

The following lemma specifies the expression of the series expansion of ψ_{ref}^u. This expression is purely formal at this stage. Convergence of the series expansion will be proved with Proposition 4.3.

Lemma 4.1. *The Spherical Surface Harmonics series expansion of* $\psi^u_{\rm ref}$ *reads*

$$\psi^u_{\rm ref}(r,\theta,\eta) = \begin{cases} \displaystyle\sum_{\ell=0}^{+\infty} \sum_{m=-\ell}^{\ell} \frac{\mu_p-1}{(\mu_p+1)\ell+1}\,\frac{r^\ell}{\varepsilon^{\ell-1}}\, g_\ell^m\, Y_\ell^m(\theta,\eta) & \text{if } r<\varepsilon \\ \displaystyle\sum_{\ell=0}^{+\infty} \sum_{m=-\ell}^{\ell} \frac{\mu_p-1}{(\mu_p+1)\ell+1}\,\frac{\varepsilon^{2+\ell}}{r^{1+\ell}}\, g_\ell^m\, Y_\ell^m(\theta,\eta) & \text{if } r\geqslant\varepsilon \end{cases}$$

where $g_\ell^m = \int_0^{2\pi}\left(\int_0^\pi g^u(\theta,\eta)\,\overline{Y_\ell^m}(\theta,\eta)\sin(\theta)\,\mathrm{d}\theta\right)\mathrm{d}\eta$ *are the coefficients of the Spherical Surface Harmonics series expansion of the source term* g^u *introduced in* (4.4).

Proof. We consider the formal series expansion (4.5) of the solution $\psi^u_{\rm ref}$ to problem (4.4). Because the magnetic potential must be bounded for $r=0$, it reads in $B(0,\varepsilon)$

$$\psi^u_{\rm ref}(r,\theta,\eta) = \sum_{\ell=0}^{+\infty}\sum_{m=-\ell}^{\ell} \alpha_\ell^m\, r^\ell\; Y_\ell^m(\theta,\eta). \tag{4.6}$$

Moreover, because the magnetic potential must tend to zero at infinity, we have in $\complement\overline{B}(0,\varepsilon)$

$$\psi^u_{\rm ref}(r,\theta,\eta) = \sum_{\ell=0}^{+\infty}\sum_{m=-\ell}^{\ell} \beta_\ell^m\, \frac{1}{r^{\ell+1}}\; Y_\ell^m(\theta,\eta). \tag{4.7}$$

The constants α_ℓ^m and β_ℓ^m are determined by the conditions across $S(0,\varepsilon)$. The continuity of $\psi^u_{\rm ref}$ implies

$$\forall \ell\in\mathbb{N}\quad \forall m\in\{-\ell,\dots,\ell\}\qquad \alpha_\ell^m = \frac{\beta_\ell^m}{\varepsilon^{2\ell+1}}\cdot \tag{4.8}$$

Let us examine the condition on the normal derivative in (4.4). From (2.14), we have for all $x\in S(0,\varepsilon)$

$$g^u(x) = -\frac{\mu_p-1}{\mu_p+2}\frac{\varepsilon^3}{|x-u|^5}\Big(3\big(e_3\cdot(x-u)\big)\,\big((x-u)\cdot n\big) - \big(e_3\cdot n\big)\,\big((x-u)\cdot(x-u)\big)\Big). \tag{4.9}$$

This function belongs to $\mathcal{C}^\infty(S(0,\varepsilon))$ and it can be expanded as a linear combination of Spherical Surface Harmonics as

$$g^u(\theta,\eta) = \sum_{\ell=0}^{+\infty}\sum_{m=-\ell}^{\ell} g_\ell^m\; Y_\ell^m(\theta,\eta) \tag{4.10}$$

where

$$g_\ell^m = \int_0^{2\pi}\left(\int_0^\pi g^u(\theta,\eta)\,\overline{Y_\ell^m}(\theta,\eta)\;\sin(\theta)\;\mathrm{d}\theta\right)\,\mathrm{d}\eta. \tag{4.11}$$

Thus, the interface condition in (4.2) is found to give rise to the relation

$$\forall \ell\in\mathbb{N}\quad \forall m\in\{-\ell,\dots,\ell\}\qquad \mu_p\alpha_\ell^m\ell\varepsilon^{\ell-1} + (\ell+1)\frac{\beta_\ell^m}{\varepsilon^{\ell+2}} = (\mu_p-1)\,g_\ell^m.$$

From (4.8), it follows that

$$\forall \ell\in\mathbb{N}\quad \forall m\in\{-\ell,\dots,\ell\}\qquad \beta_\ell^m = \frac{\mu_p-1}{(\mu_p+1)\ell+1}\varepsilon^{\ell+2}\,g_\ell^m. \tag{4.12}$$

Plugging (4.12) into (4.7) we obtain the series expansion in $\complement\overline{B}(0,\varepsilon)$. Similarly, from (4.12) and (4.8), we deduce the series expansion in $B(0,\varepsilon)$. $\square$

According to Lemma 4.1, in order to estimate the behavior of the solution ψ^u_{ref} to the reference problem (4.4), we have to control the coefficients g^m_ℓ. This is the subject of the following lemma where the notation Δ_s refers to the Laplace–Beltrami operator on the sphere:

$$\Delta_s = \frac{1}{\sin(\theta)}\partial_\theta\big(\sin(\theta)\partial_\theta\big) + \frac{1}{\sin^2(\theta)}\partial^2_\eta.$$

For all integer $p \geqslant 1$, we set $\Delta^p_s = \Delta_s \circ \cdots \circ \Delta_s$ (p times) and by convention Δ^0_s is the identity. For convenience, we also introduce the gradient operator on the sphere

$$\nabla_s = \begin{pmatrix} \dfrac{\partial}{\partial\theta} \\ \dfrac{1}{\sin(\theta)}\dfrac{\partial}{\partial\eta} \end{pmatrix}.$$

Lemma 4.2. *Coefficients g^m_ℓ for $\ell \in \mathbb{N}, m \in \{-\ell,\dots,\ell\}$ in the spherical harmonic expansion of g^u defined in (4.10) and (4.11) satisfy $g^0_0 = 0$ and for any choice of $p \in \mathbb{N}$*

$$\forall \ell \in \mathbb{N}\setminus\{0\} \quad \forall m \in \{-\ell,\dots,\ell\} \qquad |g^m_\ell| \leqslant \frac{\sqrt{4\pi}}{(\ell(\ell+1))^p}\,\|\Delta^p_s g^u\|_\infty$$

with

$$\|g^u\|_\infty \leqslant 4\frac{\mu_p - 1}{\mu_p + 2}\,\frac{\varepsilon^3}{(|u| - \varepsilon)^3}, \tag{4.13a}$$

$$\|\Delta_s g^u\|_\infty \leqslant \frac{\mu_p - 1}{\mu_p + 2}\frac{\varepsilon^3}{(|u| - \varepsilon)^5}\Big(450\varepsilon^2 + 139\varepsilon|u| + 8|u|^2\Big). \tag{4.13b}$$

Proof. Let us first show that $g^0_0 = 0$. From (4.11), we have

$$g^0_0 = -\frac{1}{\sqrt{2\pi}}\oint_{S(0,\varepsilon)} \frac{\partial\varphi_{\mathrm{ref}}}{\partial n}(x-u)\,\mathrm{d}\sigma_x = -\frac{1}{\sqrt{2\pi}}\oint_{u+S(0,\varepsilon)} \frac{\partial\varphi_{\mathrm{ref}}}{\partial n}(y)\,\mathrm{d}\sigma_y.$$

It follows from Stokes' formula that

$$g^0_0 = -\frac{1}{2\sqrt{\pi}}\int_{u+B(0,\varepsilon)} \Delta\varphi_{\mathrm{ref}}(y)\,\mathrm{d}y = 0.$$

Let us now consider the estimates of g^m_ℓ for $\ell \geqslant 1$. To highlight the decrease in coefficients with respect to ℓ, the idea is to use the fact that the elements Y^m_ℓ are eigenfunctions to the Laplacian: $\Delta_s Y^m_\ell = -\ell(\ell+1)\,Y^m_\ell$. It follows from (4.11) that

$$g^m_\ell = -\frac{1}{\ell(\ell+1)}\int_0^{2\pi}\int_0^\pi g^u(\theta,\eta)\,\Delta_s\overline{Y^m_\ell}(\theta,\eta)\,\sin(\theta)\,\mathrm{d}\theta\,\mathrm{d}\eta.$$

Since $g^u \in \mathcal{C}^\infty(S(0,\varepsilon))$, using Green's formula, we have

$$g^m_\ell = -\frac{1}{\ell(\ell+1)}\int_0^{2\pi}\int_0^\pi \Delta_s g^u(\theta,\eta)\,\overline{Y^m_\ell}(\theta,\eta)\,\sin(\theta)\;\mathrm{d}\theta\,\mathrm{d}\eta.$$

Then, repeated use of Green's formula $p-1$ more times yields

$$g^m_\ell = \frac{(-1)^p}{(\ell(\ell+1))^p}\int_0^{2\pi}\int_0^\pi \Delta^p_s g^u(\theta,\eta)\,\overline{Y^m_\ell}(\theta,\eta)\,\sin(\theta)\;\mathrm{d}\theta\,\mathrm{d}\eta.$$

It follows that

$$\begin{aligned} |g_\ell^m| &\leqslant \frac{1}{(\ell(\ell+1))^p} \int_0^{2\pi} \left(\int_0^{\pi} \left|\Delta_s^p g^u(\theta,\eta)\right| \left|\overline{Y_\ell^m}(\theta,\eta)\right| \ \sin(\theta)\ \mathrm{d}\theta \right) \ \mathrm{d}\eta \\ &\leqslant \frac{1}{(\ell(\ell+1))^p} \left\|\Delta_s^p g^u\right\|_\infty \ \int_0^{2\pi} \left(\int_0^{\pi} \left|Y_\ell^m(\theta,\eta)\right| \ \sin(\theta)\ \mathrm{d}\theta \right) \ \mathrm{d}\eta \\ &\leqslant \frac{\sqrt{4\pi}}{(\ell(\ell+1))^p} \left\|\Delta_s^p g^u\right\|_\infty. \end{aligned}$$

This complete the first part of the proof. It remains to show the two estimates (4.13a). From (4.9), we have for all $x \in S(0,\varepsilon)$

$$|g^u(x)| \leqslant 4\, \frac{\mu_p - 1}{\mu_p + 2} \frac{\varepsilon^3}{|x-u|^3}\cdot$$

The estimate (4.13) follows from the inequality: $|x-u| \geqslant |u| - |x| = |u| - \varepsilon$.

In order to obtain the estimate for $\|\Delta_s g^u\|_\infty$, we proceed as follows. We have

$$g^u(x) = -\frac{\mu_p - 1}{\mu_p + 2} \left(3 \frac{h^{\widetilde{u}}(\widetilde{x})}{|\widetilde{x} - \widetilde{u}|^5} - \frac{\left(e_3 \cdot n\right)}{|\widetilde{x} - \widetilde{u}|^3} \right) \tag{4.14}$$

where we have set $\widetilde{x} = x/\varepsilon$, $\widetilde{u} = u/\varepsilon$ and $h^{\widetilde{u}}(\widetilde{x}) = \big(e_3 \cdot (\widetilde{x} - \widetilde{u})\big)\, \big((\widetilde{x} - \widetilde{u}) \cdot n\big)$. For $p \in \mathbb{N}$, $p \geqslant 1$, we define $\forall \widetilde{x} \in S^2$ and $\forall \widetilde{u} \notin S^2$

$$G_p(\widetilde{x}, \widetilde{u}) = \frac{1}{|\widetilde{x} - \widetilde{u}|^p}\cdot$$

A simple, yet cumbersome, direct calculation shows that

$$\Delta_s G_p(\widetilde{x}, \widetilde{u}) = p(p+2) |J_s(\widetilde{x})\, \widetilde{u}|^2 \ G_{p+4}(\widetilde{x}, \widetilde{u}) - 2p\big(1 + (\widetilde{x} \cdot (\widetilde{u} - \widetilde{x}))\big) \ G_{p+2}(\widetilde{x}, \widetilde{u})$$

where $J_s(\widetilde{x})$ denotes the following 2×3 matrix

$$J_s(\widetilde{x}) = \begin{pmatrix} \cos(\theta)\cos(\eta) & \cos(\theta)\sin(\eta) & -\sin(\eta) \\ -\sin(\eta) & \cos(\eta) & 0 \end{pmatrix} = \nabla_s \widetilde{x}.$$

Moreover, we have

$$\nabla_s G_p(\widetilde{x}, \widetilde{u}) = p \left(J_s(\widetilde{x})\, \widetilde{u} \right) \ G_{p+2}(\widetilde{x}, \widetilde{u}).$$

Note that $J_s(\widetilde{x})\, \widetilde{u} = J_s(\widetilde{x})\, (\widetilde{u} - \widetilde{x})$ and $|J_s(\widetilde{x})\, \widetilde{u}| \leqslant \sqrt{2}\, |\widetilde{x} - \widetilde{u}|$. Therefore,

$$\begin{aligned} |\Delta_s G_p(\widetilde{x}, \widetilde{u})| &\leqslant 2p(p+3) \ G_{p+2}(\widetilde{x}, \widetilde{u}) + 2p \ G_{p+1}(\widetilde{x}, \widetilde{u}) \\ |\nabla_s G_p(\widetilde{x}, \widetilde{u})| &\leqslant \sqrt{2} p \, G_{p+1}(\widetilde{x}, \widetilde{u}). \end{aligned}$$

Another direct calculation shows that

$$\Delta_s h^{\widetilde{u}}(\widetilde{x}) = 2\big(1 - n \cdot (\widetilde{x} - \widetilde{u})\big) \left((\widetilde{x} - \widetilde{u}) \cdot e_3\right) - 2\big(\widetilde{x} \cdot e_3\big) \left((\widetilde{x} - \widetilde{u}) \cdot n\right) + 2\big(\partial_\theta \widetilde{x} \cdot e_3\big) \left(\partial_\theta x \cdot (\widetilde{x} - \widetilde{u})\right)$$

and

$$\nabla_s h^{\widetilde{u}}(\widetilde{x}) = \left((\widetilde{x} - \widetilde{u}) \cdot n\right) \left(J_s(\widetilde{x})\, e_3\right) - \left((\widetilde{x} - \widetilde{u}) \cdot e_3\right) \left(J_s(\widetilde{x})\, \widetilde{u}\right).$$

Because $|\widetilde{x}| = |\partial_\theta \widetilde{x}| = |\partial_\eta \widetilde{x}| = 1$, we have the estimates

$$\begin{aligned} |h^{\widetilde{u}}(\widetilde{x})| &\leqslant |\widetilde{x} - \widetilde{u}|^2 \\ |\Delta_s h^{\widetilde{u}}(\widetilde{x})| &\leqslant 2\, |\widetilde{x} - \widetilde{u}|^2 + 6\, |\widetilde{x} - \widetilde{u}| \\ |\nabla_s h^{\widetilde{u}}(\widetilde{x})| &\leqslant \sqrt{2}\, |\widetilde{x} - \widetilde{u}|^2 + |\widetilde{x} - \widetilde{u}|. \end{aligned}$$

Now, using the differential calculus formula

$$\Delta_s(f \times g) = f\,\Delta_s g + g\,\Delta_s f + 2\,\nabla_s f \cdot \nabla_s g$$

we deduce that

$$\begin{aligned}\Delta_s g^u(x) = &-\frac{\mu_p - 1}{\mu_p + 2}\Big(3h^{\widetilde{u}}(\widetilde{x})\,\Delta_s G_5(\widetilde{x},\widetilde{u}) + 3G_5(\widetilde{x},\widetilde{u})\,\Delta_s h^{\widetilde{u}}(\widetilde{x}) + 6\nabla_s G_5(\widetilde{x},\widetilde{u}) \cdot \nabla_s h^{\widetilde{u}}(\widetilde{x}) \\ &- \big(e_3 \cdot n\big)\,\Delta_s G_3(\widetilde{x},\widetilde{u}) - G_3(\widetilde{x},\widetilde{u})\,\Delta_s\big(e_3 \cdot n\big) - 2\nabla_s G_3(\widetilde{x},\widetilde{u}) \cdot \nabla_s\big(e_3 \cdot n\big)\Big).\end{aligned}$$

To get the estimate for $\Delta_s g^u(x)$ we proceed by estimating each term involved in the preceding expression:

$$\begin{aligned}|\Delta_s g^u(x)| &\leqslant \frac{\mu_p - 1}{\mu_p + 2}\Big(8G_3(\widetilde{x},\widetilde{u}) + 6(19+\sqrt{2})G_4(\widetilde{x},\widetilde{u}) + 6(46+5\sqrt{2})G_5(\widetilde{x},\widetilde{u})\Big) \\ &\leqslant \frac{\mu_p - 1}{\mu_p + 2}\,\frac{1}{|\widetilde{x}-\widetilde{u}|^5}\Big(8|\widetilde{x}-\widetilde{u}|^2 + 123|\widetilde{x}-\widetilde{u}| + 219\Big) \\ &= \frac{\mu_p - 1}{\mu_p + 2}\,\frac{\varepsilon^3}{|x-u|^5}\left(8|x-u|^2 + 123\varepsilon|x-u| + 219\varepsilon^2\right).\end{aligned}$$

From the inequalities $|x-u| \leqslant |x| + |u|$ and $|x-u| \geqslant |u| - |x| = |u| - \varepsilon$, we finally obtain (4.13a). ☐

We are now in position to prove convergence of the series expansion for ψ^u_{ref} introduced in Lemma 4.1.

Proposition 4.3. *On the one hand, the series* (4.7) *where* β^m_ℓ, $\ell \in \mathbb{N}, m \in \{-\ell,\dots,\ell\}$, *is defined in* (4.12), *converges uniformly on* $\complement\overline{B}(0,\varepsilon)$. *On the other hand, the series* (4.6) *where* α^m_ℓ, $\ell \in \mathbb{N}, m \in \{-\ell,\dots,\ell\}$, *is defined in* (4.8), *converges uniformly on* $B(0,\varepsilon)$.

Proof. Let $a_\ell(r,\theta,\eta) = \sum_{m=-\ell}^{\ell} \alpha^m_\ell\, r^\ell\; Y^m_\ell(\theta,\eta)$ be the coefficient of rank ℓ of the series (4.6). From (4.8) and (4.12), we have

$$a_\ell(r,\theta,\eta) = \frac{(\mu_p-1)\varepsilon}{(\mu_p+1)\ell+1}\left(\frac{r}{\varepsilon}\right)^\ell \sum_{m=-\ell}^{\ell} g^m_\ell\; Y^m_\ell(\theta,\eta).$$

It follows from Lemma 4.2 (considered with $p=1$) that

$$|a_\ell(r,\theta,\eta)| \leqslant \frac{\sqrt{4\pi}}{\ell(\ell+1)}\,\|\Delta_s g^u\|_\infty\,\frac{(\mu_p-1)\varepsilon}{(\mu_p+1)\ell+1}\left(\frac{r}{\varepsilon}\right)^\ell \sum_{m=-\ell}^{\ell} |Y^m_\ell(\theta,\eta)|\,. \tag{4.15}$$

Using the following estimate (see Appendix C for a proof)

$$\sum_{m=-\ell}^{\ell} |Y^m_\ell(\theta,\eta)| \leqslant \frac{3\sqrt{3}}{\sqrt{4\pi}}\,\ell^{\frac{3}{2}}, \tag{4.16}$$

we conclude that $\sum_{\ell\in\mathbb{N}} a_\ell(r,\theta,\eta)$ is uniformly convergent on $B(0,\varepsilon)$.

Similarly, let $b_\ell(r,\theta,\eta) = \sum_{m=-\ell}^{\ell} \beta^m_\ell\, \frac{1}{r^{\ell+1}}\; Y^m_\ell(\theta,\eta)$ be the coefficient of rank ℓ of the series (4.7). From (4.12), we have

$$b_\ell(r,\theta,\eta) = \frac{(\mu_p-1)\varepsilon}{(\mu_p+1)\ell+1}\left(\frac{\varepsilon}{r}\right)^{\ell+1} \sum_{m=-\ell}^{\ell} g^m_\ell\; Y^m_\ell(\theta,\eta). \tag{4.17}$$

From Lemma 4.2 and from (4.16), we deduce that

$$|b_\ell(r,\theta,\eta)| \leqslant \frac{(\mu_p-1)\varepsilon}{(\mu_p+1)\ell+1}\,\|\Delta_s g^u\|_{\infty,S(0,\varepsilon)}\,\frac{3\sqrt{3}\,\ell^{\frac{3}{2}}}{\ell(\ell+1)}\left(\frac{\varepsilon}{r}\right)^{\ell+1} \tag{4.18}$$

and we conclude that the series $\sum_{\ell\in\mathbb{N}} b_\ell(r,\theta,\eta)$ converges uniformly on $\complement\overline{B}(0,\varepsilon)$. ☐

Finally, we are in position to prove the following result for ψ^u_{ref} which is the analogue of Proposition 2.2 for φ_{ref}.

Proposition 4.4. *Let ψ^u_{ref} be the solution to problem (4.4). For all $x \in \complement\overline{B}(0,\varepsilon)$, we have*

$$\begin{aligned} |\psi^u_{\mathrm{ref}}(x)| &\leqslant 12\sqrt{3}\,\lambda_p\,\frac{\varepsilon^3}{(|u|-\varepsilon)^3}\,\frac{\varepsilon^2}{|x|}\,\mathrm{Li}_{-\frac{1}{2}}\left(\frac{\varepsilon}{|x|}\right)\\ |\nabla\psi^u_{\mathrm{ref}}(x)| &\leqslant A_4\,\lambda_p\,\frac{\varepsilon^3}{(|u|-\varepsilon)^3}\,\frac{\varepsilon^2}{|x|^2}\,\mathrm{Li}_{-\frac{3}{2}}\left(\frac{\varepsilon}{|x|}\right)\end{aligned} \tag{4.19}$$

where $\lambda_p := \dfrac{(\mu_p-1)^2}{(\mu_p+1)(\mu_p+2)} \in [0,1]$ *and* $\mathrm{Li}_s(z)$ *refers to the Polylogarithm function of order s. Moreover, the constant A_4 is such that* $A_4 \approx 59.93$.

Proof. The estimate of $\psi^u_{\mathrm{ref}}(x)$ is deduced from the Spherical Surface Harmonic series expansion given in Lemma 4.1 for $r \geqslant \varepsilon$ combined with the estimate of the coefficients g^m_ℓ given in Lemma 4.2 for $p=0$ and with (4.16). Let us consider the estimate of $\nabla\psi^u_{\mathrm{ref}}(x)$. In the spherical coordinate basis, we have

$$|\nabla\psi^u_{\mathrm{ref}}(x)|^2 = |\partial_r\psi^u_{\mathrm{ref}}(r,\theta,\eta)|^2 + |\tfrac{1}{r}\,\partial_\theta\psi^u_{\mathrm{ref}}(r,\theta,\eta)|^2 + |\tfrac{1}{r\sin(\theta)}\,\partial_\eta\psi^u_{\mathrm{ref}}(r,\theta,\eta)|^2. \tag{4.20}$$

Since $\psi^u_{\mathrm{ref}}(r,\theta,\eta) = \sum_{\ell=1}^{+\infty}\sum_{m=-\ell}^{\ell} \beta^m_\ell\,\frac{1}{r^{\ell+1}}\,Y^m_\ell(\theta,\eta)$ in $\complement\overline{B}(0,\varepsilon)$, we deduce that

$$\partial_r\psi^u_{\mathrm{ref}}(r,\theta,\eta) = -\sum_{\ell=1}^{+\infty}\sum_{m=-\ell}^{\ell} \beta^m_\ell\,\frac{\ell+1}{r^{\ell+2}}\,Y^m_\ell(\theta,\eta).$$

An estimate for $\partial_r\psi^u_{\mathrm{ref}}$ can be obtained in exactly the same way as for ψ^u_{ref}. Namely, using

- estimate (4.12) for coefficients β^m_ℓ
- estimate of the coefficients g^m_ℓ given in Lemma 4.2 considered with $p=0$

$$|g^m_\ell| \leqslant 4\sqrt{4\pi}\,\frac{\mu_p-1}{\mu_p+2}\,\frac{\varepsilon^3}{(|u|-\varepsilon)^3} \tag{4.21}$$

- estimate (4.16) on the Spherical Surface Harmonic functions Y^m_ℓ

we find that

$$|\partial_r\psi^u_{\mathrm{ref}}(r,\theta,\eta)| \leqslant 24\sqrt{3}\,\lambda_p\,\frac{\varepsilon^3}{(|u|-\varepsilon)^3}\,\frac{\varepsilon^2}{r^2}\,\mathrm{Li}_{-\frac{3}{2}}\left(\frac{\varepsilon}{r}\right)\cdot \tag{4.22}$$

Let us consider the second component of $\nabla\psi^u_{\mathrm{ref}}$ given by

$$\frac{1}{r}\partial_\theta\psi^u_{\mathrm{ref}}(r,\theta,\eta) = \sum_{\ell=1}^{+\infty}\sum_{m=-\ell}^{\ell} \beta^m_\ell\,\frac{1}{r^{\ell+2}}\,\partial_\theta Y^m_\ell(\theta,\eta).$$

Here again, using estimate (4.12) for coefficients β^m_ℓ combined with the estimate g^m_ℓ given in Lemma 4.2 considered with $p=0$ and the estimate of $\sum_{m=-\ell}^{\ell}|\partial_\theta Y^m_\ell(\theta,\eta)|$ given by (C.3) in Appendix C, we get

$$\left|\frac{1}{r}\partial_\theta\psi^u_{\mathrm{ref}}(r,\theta,\eta)\right| \leqslant 4\sqrt{6}(1+\pi)\,\lambda_p\,\frac{\varepsilon^3}{(|u|-\varepsilon)^3}\,\frac{\varepsilon^2}{r^2}\,\mathrm{Li}_{-\frac{3}{2}}\left(\frac{\varepsilon}{r}\right)\cdot \tag{4.23}$$

The third component of $\nabla\psi^u_{\mathrm{ref}}$ is given by

$$\frac{1}{r\sin(\theta)}\,\partial_\eta\psi^u_{\mathrm{ref}}(r,\theta,\eta) = \sum_{\ell=1}^{+\infty}\sum_{m=-\ell}^{\ell} \beta^m_\ell\,\frac{1}{r^{\ell+2}}\,\frac{1}{\sin(\theta)}\,\partial_\eta Y^m_\ell(\theta,\eta).$$

Proceeding as before using now the estimate of $\sum_{m=-\ell}^{\ell}\left|\frac{1}{\sin(\theta)}\,\partial_\eta Y_\ell^m(\theta,\eta)\right|$ given by (C.4) in Appendix C, we get

$$\left|\frac{1}{r\sin(\theta)}\partial_\eta \psi_{\mathrm{ref}}^u(r,\theta,\eta)\right| \leqslant 6\sqrt{6}\,\lambda_p\,\frac{\varepsilon^3}{(|u|-\varepsilon)^3}\,\frac{\varepsilon^2}{r^2}\,\mathrm{Li}_{-\frac{3}{2}}\left(\frac{\varepsilon}{r}\right). \tag{4.24}$$

Finally, combining (4.22), (4.23) and (4.24) together with (4.20), we conclude that

$$|\nabla\psi_{\mathrm{ref}}^u(x)| \leqslant A_4\,\lambda_p\,\frac{\varepsilon^3}{(|u|-\varepsilon)^3}\,\frac{\varepsilon^2}{|x|^2}\,\mathrm{Li}_{-\frac{3}{2}}\left(\frac{\varepsilon}{|x|}\right), \tag{4.25}$$

where $A_4=\sqrt{(24\sqrt{3})^2+(4\sqrt{6}(1+\pi))^2+(6\sqrt{6})^2}=2\sqrt{6(85+8\pi+4\pi^2)}\approx 59.93.$ □

4.3. $\mathbb{W}^1$-estimate of the error when taking into account pairwise interactions

When the approximation $\varphi\approx\sum_{j=1}^N\varphi_{c_j}$ is not accurate enough, a more accurate approximate solution can be obtained by using the two terms expansion

$$\varphi=\sum_{j=1}^N\varphi_{c_j}+\sum_{j=1}^N\sum_{\substack{k=1\\k\neq j}}^N\varphi_{c_k,c_j}+\chi \tag{4.26}$$

where χ denotes the approximation error.

Proposition 4.5. *The remainder χ in (4.26) satisfies*

$$\begin{cases}\Delta\chi &=0 & \text{in} & \Omega_1,\ldots,\Omega_N \text{ and } \Omega^c\\ \left[\mu\dfrac{\partial\chi}{\partial n}\right] &=[\mu]\,g_1 & \text{across} & \Sigma_1,\ldots,\Sigma_N\end{cases} \tag{4.27}$$

where the source term g_1 defined by

$$\forall x\in\Sigma_i\qquad g_1(x)=-\sum_{\substack{j=1\\j\neq i}}^N\sum_{\substack{k=1\\k\neq j}}^N\nabla\varphi_{c_k-c_j,0}(T_{c_j}(x))\cdot n(x)$$

is such that

$$\|g_1\|_{\mathbb{L}^\infty(\Sigma)}\leqslant A_4\,\lambda_p\left(\frac{2\varepsilon}{\delta}\right)^5\left(B_3+3\ln\left(\frac{2}{\delta}\right)\right)\left(B_3\,\mathrm{Li}_{-\frac{3}{2}}\left(\frac{2\varepsilon}{\delta}\right)+3\left(\frac{2\varepsilon}{\delta}\right)\ln\left(\frac{2}{\delta}\right)\right). \tag{4.28}$$

Proof. Since the functions φ, φ_{c_j} and φ_{c_k,c_j} for $j,k\in\{1,\ldots,N\}$, $k\neq j$, all satisfy the Laplace equation in each domain Ω_i, $i\in\{1,\ldots,N\}$ and in Ω^c, it follows from (4.26) by linearity that χ also satisfies the Laplace equation. Moreover, for all $i\in\{1,\ldots,N\}$ we have

$$\left[\mu\frac{\partial\chi}{\partial n}\right]=\left[\mu\frac{\partial\psi}{\partial n}\right]-\sum_{j=1}^N\sum_{\substack{k=1\\k\neq j}}^N\left[\mu\frac{\partial\varphi_{c_k,c_j}}{\partial n}\right]\ \text{across }\Sigma_i. \tag{4.29}$$

From (3.2), (3.3) and (4.2), we can express the interface condition (4.29) across Σ_i as

$$\left[\mu\frac{\partial\chi}{\partial n}\right]=\underbrace{[\mu]\,g_0-\sum_{\substack{k=1\\k\neq i}}^N\left[\mu\frac{\partial\varphi_{c_k,c_i}}{\partial n}\right]}_{=0}-\sum_{\substack{j=1\\j\neq i}}^N\sum_{\substack{k=1\\k\neq j}}^N\left[\mu\frac{\partial\varphi_{c_k,c_j}}{\partial n}\right]. \tag{4.30}$$

The potential φ_{c_k,c_j} solution to problem (4.2) is continuous in $\mathbb{R}^3$ and has regularity $\mathcal{C}^\infty$ everywhere except on the boundary Σ_j. Therefore, as soon as $|c_i - c_j| > 2\varepsilon$ (that corresponds to the fact that the particles Ω_i and Ω_j of radius ε do not intersect) the normal derivative $\frac{\partial \varphi_{c_k,c_j}}{\partial n}$ is continuous across Σ_i and (4.30) reads

$$\left[\mu \frac{\partial \chi}{\partial n}\right] = -[\mu] \sum_{\substack{j=1\\ j\neq i}}^{N} \sum_{\substack{k=1\\ k\neq j}}^{N} \frac{\partial \varphi_{c_k,c_j}}{\partial n} = -[\mu] \sum_{\substack{j=1\\ j\neq i}}^{N} \sum_{\substack{k=1\\ k\neq j}}^{N} \left(\nabla \varphi_{c_k - c_j,0} \circ T_{c_j}\right) \cdot n. \tag{4.31}$$

The first result stated in the lemma is proven. In order to obtain the estimate on the source term g_1, we start with

$$\forall i \in \{1,\dots,N\} \quad \forall x \in \Sigma_i \qquad |g_1(x)| \leqslant \sum_{\substack{j=1\\ j\neq i}}^{N} \sum_{\substack{k=1\\ k\neq j}}^{N} |\nabla \psi_{\mathrm{ref}}^{c_k - c_j}(x - c_j)|.$$

We deduce from Proposition 4.4 that

$$|g_1(x)| \leqslant A_4\, \lambda_p \sum_{\substack{j=1\\ j\neq i}}^{N} \sum_{\substack{k=1\\ k\neq j}}^{N} \frac{\varepsilon^5}{(|c_k - c_j| - \varepsilon)^3 |c_j - x|^2}\ \mathrm{Li}_{-\frac{3}{2}}\left(\frac{\varepsilon}{|c_j - x|}\right).$$

From the definition of the Polylogarithm function and the inequality $|c_k - c_j| - \varepsilon \geqslant \frac{1}{2}|c_k - c_j|$, it follows that

$$|g_1(x)| \leqslant A_4\, \lambda_p \sum_{\ell=1}^{+\infty} \ell^{\frac{3}{2}} \varepsilon^{\ell+2} \sum_{\substack{j=1\\ j\neq i}}^{N} \frac{1}{|c_j - x|^{\ell+2}} \sum_{\substack{k=1\\ k\neq j}}^{N} \frac{\varepsilon^3}{|c_k - c_j|^3}.$$

Using relation (B.1) of Appendix B, we can bound the last sum to obtain

$$|g_1(x)| \leqslant A_4\, \lambda_p \left(\frac{2\varepsilon}{\delta}\right)^3 \left(B_3 + 3\ln\left(\frac{2}{\delta}\right)\right) \sum_{\ell=1}^{+\infty} \ell^{\frac{3}{2}} \varepsilon^{\ell+2} \sum_{\substack{j=1\\ j\neq i}}^{N} \frac{1}{|c_j - x|^{\ell+2}}.$$

Finally, using relations (B.1) and (B.2) of Appendix B, we can bound the sums $\sum_{\substack{j=1\\ j\neq i}}^{N} \frac{1}{|c_j - x|^{\ell+2}}$ and for all $\ell \geqslant 1$ to conclude that

$$|g_1(x)| \leqslant A_4\, \lambda_p \left(\frac{2\varepsilon}{\delta}\right)^5 \left(B_3 + 3\ln\left(\frac{2}{\delta}\right)\right) \left(B_3\, \mathrm{Li}_{-\frac{3}{2}}\left(\frac{2\varepsilon}{\delta}\right) + 3\left(\frac{2\varepsilon}{\delta}\right) \ln\left(\frac{2}{\delta}\right)\right).$$

□

Following the same steps as in the proof of Theorem 3.3, we deduce a $\mathbb{W}^1$-estimate of the remainder χ defined in (4.26).

Theorem 4.6. *Let $\Omega_1, \dots, \Omega_N$ be N isolated spherical particles in $B(0,1) \subset \mathbb{R}^3$, centered respectively at c_j, $j \in \{1,\dots,N\}$ with the same radius ε. For all $j,k \in \{1,\dots,N\}, j \neq k$, let $\varphi_{c_j} \in \mathbb{W}_0^1(\mathbb{R}^3)$ be the solution to problem (2.17) and $\varphi_{c_k,c_j} \in \mathbb{W}_0^1(\mathbb{R}^3)$ be the solution to problem (4.2). We have*

$$\left\| \varphi - \left(\sum_{j=1}^{N} \varphi_{c_j} + \sum_{j=1}^{N} \sum_{\substack{k=1\\ k\neq j}}^{N} \varphi_{c_k,c_j} \right) \right\|_{\mathbb{W}^1(\mathbb{R}^3)} \leqslant A_1\, A_4\, (\mu_p - 1)\, \lambda_p\, N\, \varepsilon^{\frac{3}{2}} \left(\frac{2\varepsilon}{\delta}\right)^5$$
$$\times \left(B_3 + 3\ln\left(\frac{2}{\delta}\right)\right) \left(B_3\, \mathrm{Li}_{-\frac{3}{2}}\left(\frac{2\varepsilon}{\delta}\right) + 3\left(\frac{2\varepsilon}{\delta}\right) \ln\left(\frac{2}{\delta}\right)\right) \tag{4.32}$$

where δ is the minimal distance between two particles as defined in (1.1) and the constants A_1, A_4, B_3 have been explicitly estimated and are summarized in Table E.1 on page 1108.

Remark 4.7. When $\frac{2\varepsilon}{\delta}$ becomes small, since $\mathrm{Li}_{-\frac{3}{2}}(z) \sim_0 z$, estimate (4.32) reads

$$\left\| \varphi - \left(\sum_{j=1}^{N} \varphi_{c_j} + \sum_{j=1}^{N} \sum_{\substack{k=1 \\ k \neq j}}^{N} \varphi_{c_k,c_j} \right) \right\|_{\mathbb{W}^1(\mathbb{R}^3)} \lesssim (\mu_p - 1)\, \lambda_p\, N\, \varepsilon^{\frac{3}{2}} \left(\frac{2\varepsilon}{\delta} \right)^6 \left(1 + \ln \left(\frac{2}{\delta} \right) \right)^2$$

and this new bound is the product of a term $N\,\varepsilon^{\frac{3}{2}}$ of the order of φ, and the square of the first order error $\left(\frac{2\varepsilon}{\delta}\right)^3 \left(1 + \ln\left(\frac{2}{\delta}\right)\right)$.

The asymptotic regime $\varepsilon \to 0$ is particularly interesting. In the $\mathbb{W}^1$-norm, the solution φ is of order $\varepsilon^{\frac{3}{2}}$. The $\mathbb{W}^1$-error under the "non-interacting assumption" is of order $\varepsilon^{\frac{3}{2}+3}$ whereas the $\mathbb{W}^1$-error when taking into account "pairwise interactions" is of order $\varepsilon^{\frac{3}{2}+6}$. Considering a vanishing critical distance δ deteriorates the estimates, as it is expected, even if $2\varepsilon < \delta$: In this case the estimates critically depend on the magnitude of the density $2\varepsilon/\delta$.

4.4. $\mathbb{L}^\infty$-estimate of the error when taking into account pairwise interactions

Let us now prove a $\mathbb{L}^\infty$-estimate of the remainder χ defined in (4.26).

Theorem 4.8. *Let $\Omega_1, \ldots, \Omega_N$ be N isolated spherical particles in $B(0,1) \subset \mathbb{R}^3$, centered respectively at c_j, $j \in \{1, \ldots, N\}$, with the same radius ε. Let δ be the minimal distance between two particles as defined in (1.1). For all $j, k \in \{1, \ldots, N\}, i \neq k$, let $\varphi_{c_j} \in \mathbb{W}_0^1(\mathbb{R}^3)$ be the solution to problem (2.17) and $\varphi_{c_k,c_j} \in \mathbb{W}_0^1(\mathbb{R}^3)$ be the solution to problem (4.2). For all $x \in \Omega^c$, we have*

$$\left| \varphi(x) - \left(\sum_{j=1}^{N} \varphi_{c_j}(x) + \sum_{j=1}^{N} \sum_{\substack{k=1 \\ k \neq j}}^{N} \varphi_{c_k,c_j}(x) \right) \right| \leqslant (\mu_p - 1) A_4\, \lambda_p \left(\frac{2\varepsilon}{\delta} \right)^5 \left(B_3 + 3 \ln \left(\frac{2}{\delta} \right) \right)$$
$$\times \left(B_3\, \mathrm{Li}_{-\frac{3}{2}} \left(\frac{2\varepsilon}{\delta} \right) + 3 \left(\frac{2\varepsilon}{\delta} \right) \ln \left(\frac{2}{\delta} \right) \right) \times \left(B_1 \left(\frac{2}{\delta} \right)^3 \varepsilon^2 + M_x \varepsilon + A_1 A_2 (\mu_p - 1) N \left(B_2 \Big(\frac{2\varepsilon}{\delta} \Big)^3 + M_x A_3 \varepsilon^3 \right) \right)$$

where $M_x \leqslant \min(64, N)$ corresponds to the number of particles whose distance at x is less than 2δ, $\lambda_p := \frac{(\mu_p-1)^2}{(\mu_p+1)(\mu_p+2)} \in [0,1]$ and $A_1, A_2, A_3, , A_4, B_1, B_2, B_3$ are positive constants (see Tab. E.1, p. 1108 for their full expressions and values).

Proof. The remainder $\chi = \varphi - (\sum_{j=1}^N \varphi_{c_j} + \sum_{j=1}^N \sum_{\substack{k=1 \\ k \neq j}}^N \varphi_{c_k,c_j})$ satisfies (4.27) and therefore can be expressed, for all $x \in \Omega^c$, as ([6], Thm. 2, p. 120)

$$\chi(x) = -(\mu_p - 1) \sum_{j=1}^{N} \left(\int_{\Sigma_j} g_1(y)\, \mathcal{G}(x,y)\ \mathrm{d}y - \int_{\Sigma_j} \chi(y)\, \partial_n \mathcal{G}(x,y)\ \mathrm{d}y \right) \tag{4.33}$$

where $\mathcal{G}$, the Green kernel of the Laplacian in $\mathbb{R}^3$. It follows that

$$|\chi(x)| \leqslant (\mu_p - 1) \sum_{j=1}^{N} \Big(\|g_1\|_{\mathbb{L}^\infty(\Sigma_j)} \|\mathcal{G}(x,\cdot)\|_{\mathbb{L}^1(\Sigma_j)} + \|\chi\|_{\mathbb{L}^4(\Sigma_j)} \|\partial_n \mathcal{G}(x,\cdot)\|_{\mathbb{L}^{\frac{4}{3}}(\Sigma_j)} \Big). \tag{4.34}$$

Using estimate (2.10) combined with the Sobolev embedding inequality (A.4) proved in Appendix A, we obtain

$$\|\chi\|_{\mathbb{L}^4(\Sigma_j)} \leqslant A_1 A_2\, (\mu_p - 1)\, N\, \varepsilon^{\frac{3}{2}}\, \|g_1\|_{\mathbb{L}^\infty(\Sigma_j)}. \tag{4.35}$$

Then using the estimates (4.28) for $\|g_1\|_{\mathbb{L}^\infty(\Sigma)}$, (3.14a) for $\|\mathcal{G}(x,\cdot)\|_{\mathbb{L}^1(\Sigma_j)}$, (3.14b) for $\|\partial_n \mathcal{G}(x,\cdot)\|_{\mathbb{L}^{\frac{4}{3}}(\Sigma_j)}$, we get

$$\left|\chi(x)\right| \leqslant (\mu_p - 1)\|g_1\|_{\mathbb{L}^\infty(\Sigma)} \left(B_1 \left(\frac{2}{\delta}\right)^3 \varepsilon^2 + M_x \varepsilon + A_1 A_2 (\mu_p - 1) N \varepsilon^{\frac{3}{2}} \left(B_2 \left(\frac{2}{\delta}\right)^3 \varepsilon^{\frac{3}{2}} + M_x A_3 \varepsilon^{\frac{3}{2}} \right) \right) \tag{4.36}$$

where

$$\|g_1\|_{\mathbb{L}^\infty(\Sigma)} \leqslant A_4\, \lambda_p \left(\frac{2\varepsilon}{\delta}\right)^5 \left(B_3 + 3 \ln\left(\frac{2}{\delta}\right) \right) \left(B_3 \operatorname{Li}_{-\frac{3}{2}}\left(\frac{2\varepsilon}{\delta}\right) + 3 \left(\frac{2\varepsilon}{\delta}\right) \ln\left(\frac{2}{\delta}\right) \right).$$

By combining these two inequalities, we obtain the estimate. □

In the asymptotic regime $\varepsilon \to 0$, the $\mathbb{L}^\infty$-error under the "non-interacting assumption" is of order ε^4 whereas the $\mathbb{L}^\infty$-error when taking into account "pairwise interactions" is of order ε^7. Here again, considering a vanishing critical distance δ deteriorates the estimates, as it is expected, even if $2\varepsilon < \delta$: In this case the estimates critically depend on the magnitude of the density $2\varepsilon/\delta$.

5. Numerical investigations

Based on the mathematical investigations conducted in the previous sections, we have developed a basic computer program under Matlab to compute the magnetic potential φ solution to problem (2.4). The computer program offers the possibility to compute the magnetic potential with either one term or two terms in the series expansion corresponding respectively to the results stated in Theorem 3.3 and in Theorem 4.6. Computation of the first term in the expansion given by $\sum_{j=1}^N \varphi_{c_j}$ is straightforward since $\varphi_{c_j} = \varphi_{\mathrm{ref}} \circ T_{c_j}$ and the expression of φ_{ref} is given by (2.13). Computation of the second term $\sum_{j=1}^N \sum_{\substack{k=1\\k\neq j}}^N \varphi_{c_k,c_j}$, where $\varphi_{c_k,c_j} = \psi_{\mathrm{ref}}^{c_k-c_j} \circ T_{c_j}$, that takes into account pairwise interaction relies on the series expansion given by Lemma 4.1. Namely, for all $x \in \mathbb{R}^3$

$$\psi_{\mathrm{ref}}^{c_k-c_j}(x) = \begin{cases} \displaystyle\sum_{\ell=1}^{+\infty} \left(\frac{r}{\varepsilon}\right)^\ell \sum_{m=-\ell}^{\ell} \gamma_\ell^m\, Y_\ell^m(\theta,\eta) & \text{if } |x - c_j| \leqslant \varepsilon \\ \displaystyle\sum_{\ell=1}^{+\infty} \left(\frac{\varepsilon}{r}\right)^{\ell+1} \sum_{m=-\ell}^{\ell} \gamma_\ell^m\, Y_\ell^m(\theta,\eta) & \text{if } |x - c_j| > \varepsilon \end{cases} \tag{5.1}$$

where (r,θ,η) refers to the spherical coordinates of x with respect to the a frame with origin c_j and where we have set

$$\gamma_\ell^m = \frac{(\mu_p - 1)\,\varepsilon}{(\mu_p+1)\ell+1} \int_0^{2\pi} \left(\int_0^\pi g^{c_k-c_j}(\theta,\eta)\, \overline{Y_\ell^m}(\theta,\eta)\ \sin(\theta)\ \mathrm{d}\theta \right) \mathrm{d}\eta \tag{5.2}$$

and

$$g^{c_k-c_j} = -\left(\nabla\varphi_{\mathrm{ref}} \circ T_{c_k-c_j}\right) \cdot n. \tag{5.3}$$

Of course, in a numerical approach, the series expansions (5.1) have to be truncated to an integer L and the efficiency of the method depends on the convergence to zero of the series coefficients γ_ℓ^m as ℓ increases to infinity. This is discussed below.

5.1. Convergence toward zero of the series coefficients

In order to illustrate the convergence to 0 of the coefficients γ_ℓ^m given by (5.2) as ℓ tends to infinity, we have depicted in Figure 4 the values $|\gamma_\ell^m|$ for $m \in \{-\ell,\ldots,\ell\}$ and $\ell \in \{0,\ldots,18\}$ for $\mu_p = 10$, $\varepsilon = 1$ and $u = c_k - c_j = (2,1,1)^\top$. We have also depicted in Figure 5 the decimal logarithm of $\max_{m=-\ell,\ldots,\ell} |\gamma_\ell^m|$ for $\ell \in \{1,\ldots,18\}$. The slope of the straight line is approximately -0.35. This means that from ℓ to $\ell+1$ the maximal value $\max_{m=-\ell,\ldots,\ell} |\gamma_\ell^m|$ is divided by 2.23.

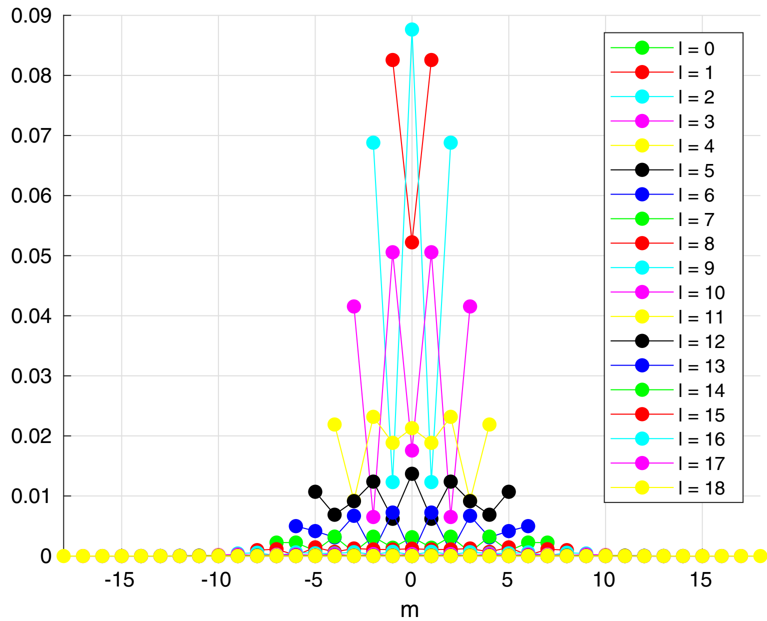

FIGURE 4. Values of $|\gamma_\ell^m|$ for $m \in \{-\ell, \dots, \ell\}$ and $\ell \in \{0, \dots, 18\}$ for $\mu_p = 10$, $\varepsilon = 1$ and $u = c_k - c_j = (2, 1, 1)^\top$.

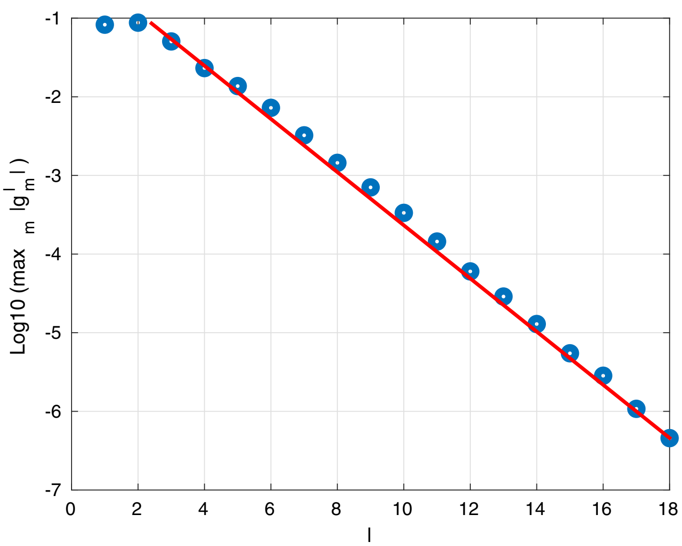

FIGURE 5. Values of the decimal logarithm of $\max_{m=-\ell,\dots,\ell} |\gamma_\ell^m|$ for $\ell = 1, \dots, 18$ for $\mu_p = 10$, $\varepsilon = 1$ and $u = c_k - c_j = (2, 1, 1)^\top$. The slope of the straight line is approximately -0.35.

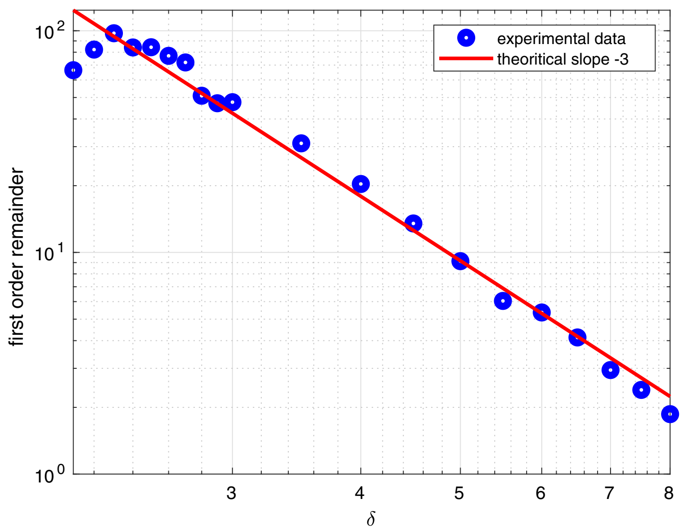

FIGURE 6. Values of $\mathfrak{E}$ as a function of the distance δ (in mm) between the two spherical particles in a log-scale. The slope of the solid line is -3.

5.2. Illustration of the mathematical results

We start with an illustration of the behavior of the bound in the estimate provided in Theorem 3.6. We consider two spherical particles ($N = 2$) with radius $\varepsilon = 1\,\mathrm{mm}$ aligned in the e_1 direction. We set

$$\mathfrak{E} := \max_{x\in\mathbb{R}^3} \left| \varphi(x) - \sum_{j=1}^{2} \varphi_{c_j}(x) \right|. \tag{5.4}$$

We have computed $\mathfrak{E}$ considering two particles at various distance δ form each other for $\mu_p = 10$ and $H_0 = \frac{1}{\mu_0}\begin{pmatrix}1 & 0 & 0\end{pmatrix}^\top$ H.m^{-1}. We have depicted in Figure 6 the quantity $\mathfrak{E}$ as a function of the distance δ between the two spherical particles in log-scale. One can observe that $\mathfrak{E}$ varies as $1/\delta^3$ as predicted by Theorem 3.6.

We then consider two spherical particles ($N = 2$) with radius ε aligned in the e_1 direction with centers at a distance $\delta = 11\,\mathrm{mm}$. We have computed $\mathfrak{E}$ considering various radius ε for $\mu_p = 10$ and $H_0 = \frac{1}{\mu_0}\begin{pmatrix}1 & 0 & 0\end{pmatrix}^\top$ H.m^{-1}. We have depicted in Figure 7 the quantity $\mathfrak{E}$ as a function of the radius ε of the two spherical particles in log-scale. One can observe that $\mathfrak{E}$ varies as ε^4 as predicted by Theorem 3.6. By linear least-square interpolation, the vertical intercept is found to be 1.053865×10^3. In the estimate provided in Theorem 3.6, for $\delta = 1$ mm, the first term in the series expansion in ε is $16\frac{(\mu_p-1)^2}{\mu_p+2}\,(B_3 + 3\,\ln 2)\,M_x \leqslant 2.8 \times 10^5$ since $M_x \leqslant N = 2$. The bound provided in Theorem 3.6 is therefore not a sharp bound in this particular case.

5.3. Numerical experiments

As a first numerical experiment, we consider the case of two spherical particles with magnetic permeability $\mu_p = 10$ and radius $\varepsilon = 1\,\mathrm{mm}$ subjected to a magnetic field aligned with the ball centers with intensity $H_0 = \frac{1}{\mu_0}$ H.m^{-1}. The two ball centers are separated by $\delta = 3\,\mathrm{mm}$, *i.e.* the two spheres are at a distance of one radius. The plane of reference ($\mathcal{P}$) where the magnetic potential is computed is a plane passing through the ball centers with size 9ε along the y-axis and 4ε along the x-axis. We have depicted in Figure 8 the potential $\varphi^{[1]} = \varphi_{c_1} + \varphi_{c_2}$ corresponding to the first term in our series expansion, *i.e.* obtained by neglecting interaction between the balls, the potential $\varphi_{c_1,c_2} + \varphi_{c_2,c_1}$ corresponding to the second term in the series expansion, *i.e.*

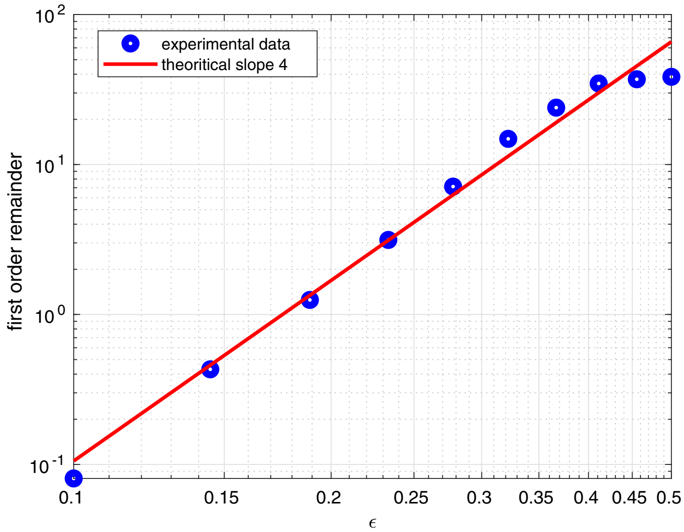

FIGURE 7. Values of $\mathfrak{E}$ as a function of the radius ε (in mm) of the two spherical particles in a log-scale. The slope of the solid line is 4.

corresponding to the pairwise interactions between the two balls and the second order series approximation of the magnetic potential $\varphi^{[2]} = \varphi_{c_1} + \varphi_{c_2} + \varphi_{c_1,c_2} + \varphi_{c_2,c_1}$. These three quantities were computed over a grid of $K = 50 \times 100$ points P_k in the plane of reference $(\mathcal{P})$ and the series expansion (5.1) has been truncated to the index $L = 16$. Computation time (CPU time) was 51.03 s under MATLAB (R2018a) on an Intel i5 Quad Core desktop computer. In this first test case, one can see that the second term in the series expansion that takes into account pairwise interactions between the two balls amounts to around 7 % of the total magnetic potential.

In order to validate our computer program based on the series expansion presented in the paper, we have also compared the second order series approximation of the magnetic potential $\varphi^{[2]} = \varphi_{c_1} + \varphi_{c_2} + \varphi_{c_1,c_2} + \varphi_{c_2,c_1}$ to the magnetic potential φ computed by the Finite Element Method (FEM) using the free software FREEFEM++ [11]. Note that the solution provided by the FEM is to be considered as a reference solution. It is not the exact solution because of the discretization error (the magnetic potential is approached by Lagrange type 2 Finite Element on a fine triangulation mesh of the computational domain) and the need to bound the computational domain by introducing an artificial boundary and a (approximate) boundary condition that takes account of the behavior of the magnetic potential at infinity. The relative maximal error over the computational grid defined by the points $P_k, k \in \{1, \dots, K\}$, on the plane of reference $(\mathcal{P})$ between the FEM solution and the solution computed by the two terms series expansion was found to be 0.67% whereas the relative discrete $\mathbb{L}^2$-error $\mathrm{err}_{\mathbb{L}^2}$ defined as

$$\mathrm{err}_{\mathbb{L}^2}^2 = \frac{\iint_{\mathcal{P}} |\varphi^{[2]}(x) - \varphi_{\mathrm{FEM}}(x)|^2 \, \mathrm{d}x}{\iint_{\mathcal{P}} |\varphi_{\mathrm{FEM}}(x)|^2 \, \mathrm{d}x} \approx \frac{\sum_{k=1}^{K} |\varphi^{[2]}(P_k) - \varphi_{\mathrm{FEM}}(P_k)|^2}{\sum_{k=1}^{K} |\varphi^{[2]}(P_k)|^2}$$

was 0.63%. For the sake of completeness, we should add that comparing the FEM solution to the solution $\varphi_{c_1} + \varphi_{c_2}$ obtained under the non-interaction assumption we obtain a relative maximal error of 5.78% and a relative $\mathbb{L}^2$ error of 5.18%. Thus, in this test example, we can conclude that taking into account pairwise interactions significantly improves the accuracy.

To go further in the numerical investigations, we have computed the relative maximal error and the relative $\mathbb{L}^2$ error for various values of the parameter δ/ε when only one term in the potential series expansion is taken into account (this corresponds to the "non-interacting assumption" case) and when the first two terms are taken into account (this corresponds to the "pairwise interactions" case). One can see on the results given in Table 1

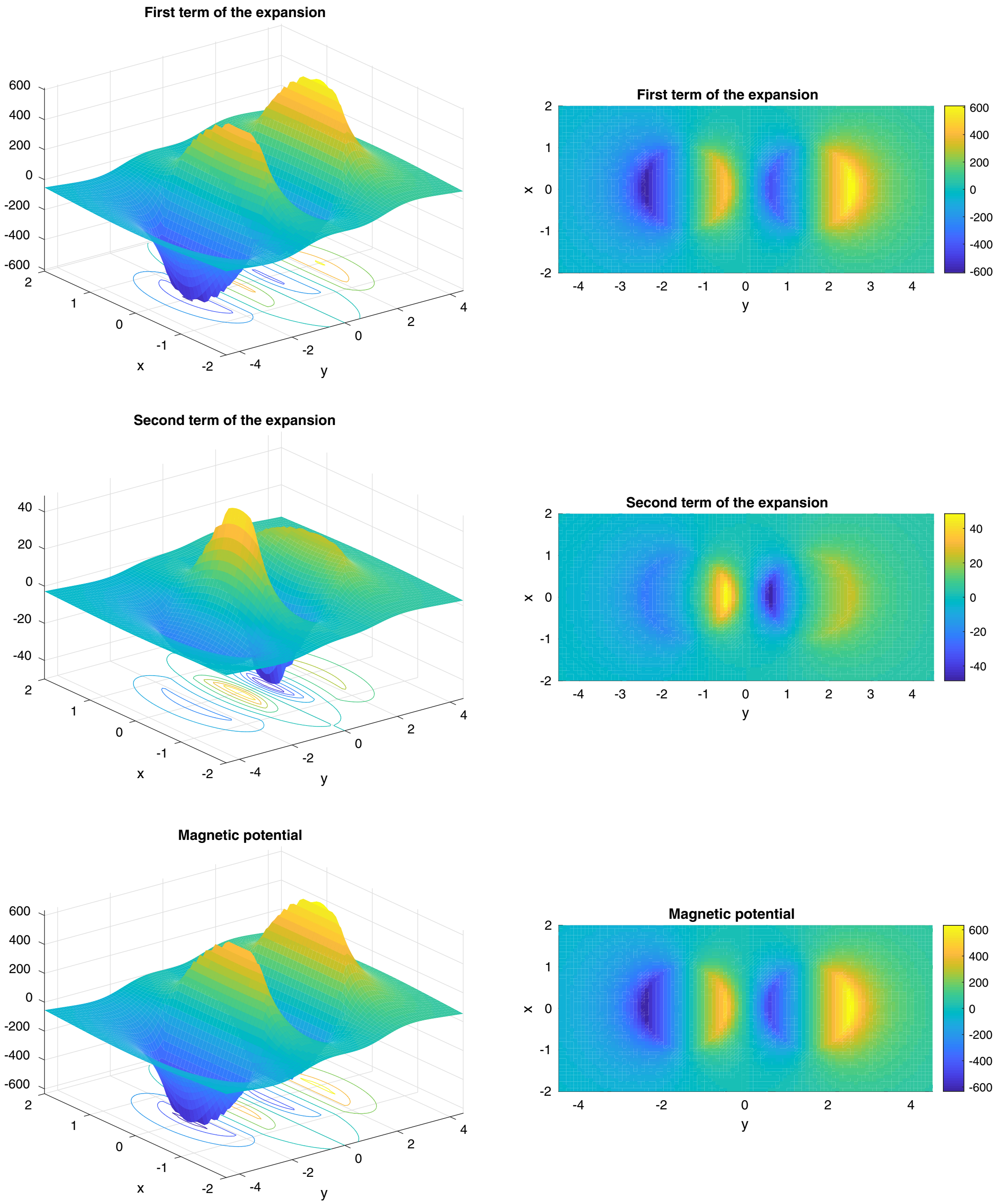

FIGURE 8. Two particles. *From top to bottom*: First term in the series expansion of the magnetic potential, second term in the series expansion and approximation of the magnetic potential obtained by summing the first two terms of the series expansion. *From left to right*: Three-dimensional shaded surface representation and two-dimensional representation of the three quantities.

TABLE 1. Relative maximal error and relative $\mathbb{L}^2$ error obtained when using one and two terms in the magnetic potential series expansion as a function of $\frac{\delta}{\varepsilon}$, *i.e.* as a function of the distance between the two ball centers.

	δ/ε	2.25	2.5	3	4	5	6	7
1 term	Max. error (%)	16.34	11.08	5.78	1.95	0.77	0.62	0.65
	$\mathbb{L}^2$error (%)	14.62	9.76	5.18	1.75	0.73	0.47	0.61
2 terms	Max. error (%)	3.07	1.23	0.67	0.71	0.71	0.77	0.82
	$\mathbb{L}^2$ error (%)	2.46	1.05	0.63	0.86	0.89	0.73	0.95

Notes. Note that for $\frac{\delta}{\varepsilon} = 2$, the balls are touching each other.

that when the two ball centers are at a distance lower than 5ε, the error made on the computation of the magnetic potential assuming that the particles have no magnetic interaction lead to a significant error. On the contrary, taking into account pairwise interactions provide good results with an error about one percent. One can also observe that when the particles become very close to each other, the error obtained with two terms in the potential series expansion tends to increase. In our test example, it is around 3% when the particles are at a distance of a quarter of their radius. This indicates that when the particles are very close to each other, taking into account pairwise interactions is not sufficient and higher order mutual interactions terms should be computed.

As a second test example, we have considered a cube of $4^3 = 64$ balls with radius $\varepsilon = 1\,\text{mm}$ regularly spaced with a distance between their centers $\delta = 3\,\text{mm}$. The balls are subjected to a magnetic field aligned with the x-direction with intensity $H_0 = \frac{1}{\mu_0}\,\text{H.m}^{-1}$. We have depicted in Figure 9 the same three potentials as in Figure 8. These three quantities were computed on 100^2 equidistant points on a square grid with size 15ε in a plane passing through the center of the cube with basis vectors corresponding to the x and y directions. Computations lasted 59 872 s. (approx. 16h30) to compute the $64 \times 63 = 4032$ particles pairwise interactions. In this test example, the second term of the series expansion is about 3.5 % of the first term. The rather important simulation time observed in this simulation can be explained by the fact our basic Matlab program is not optimized, see the next section for details .

5.4. Discussion

Let us discuss the main features of the numerical method based on the computation of pairwise interactions. For a distribution of N particles, computation of the first term $\sum_{j=1}^{N} \varphi_{c_j}$ in the expansion corresponding to the non-interaction assumption is straightforward since $\varphi_{c_j} = \varphi_{\text{ref}} \circ T_{c_j}$ and the expression of φ_{ref} is given by (2.13). The cost of this computation proportional to N is negligible compared to the computational cost of pairwise interactions proportional to N^2. Computation of the second term in the expansion $\sum_{j=1}^{N} \sum_{\substack{k=1 \\ k \neq j}}^{N} \varphi_{c_k,c_j}$, where $\varphi_{c_k,c_j} = \psi_{\text{ref}}^{c_k - c_j} \circ T_{c_j}$, corresponding to pairwise interactions, requires the evaluation of $\psi_{\text{ref}}^{c_k - c_j}$ given by formula (5.1) a number of times equal to $N(N-1)$. The series expansion (5.1) must be truncated at a order L. Numerical experiments shown that the series coefficients γ_ℓ^m decrease rather quickly and truncating the series expansion to $L \approx 20$ provides satisfactory results. For each pair of particles, we have $L(L+2)$ coefficients γ_ℓ^m to compute using formula (5.2) that each necessitates the evaluation of a double integral. The computation of series expansion (5.1) must be repeated for each point in $\mathbb{R}^3$ where the magnetic field is to be computed. However, one the one hand, the coefficients γ_ℓ^m are independents of the point $x \in \mathbb{R}^3$ where the magnetic field is to be computed. Therefore, they can be computed once and for all for a given particles distribution. Moreover, the double integral involved in the definition (5.2) of γ_ℓ^m can be computed by fast spherical Fourier algorithms [16, 24]. On the other hand, the Spherical Harmonics functions Y_ℓ^m involved in the series expansion (5.1) depend on the point $x \in \mathbb{R}^3$ where the magnetic field is to be computed but are independent of the particles distribution. Therefore, they can be computed once and for all for each point

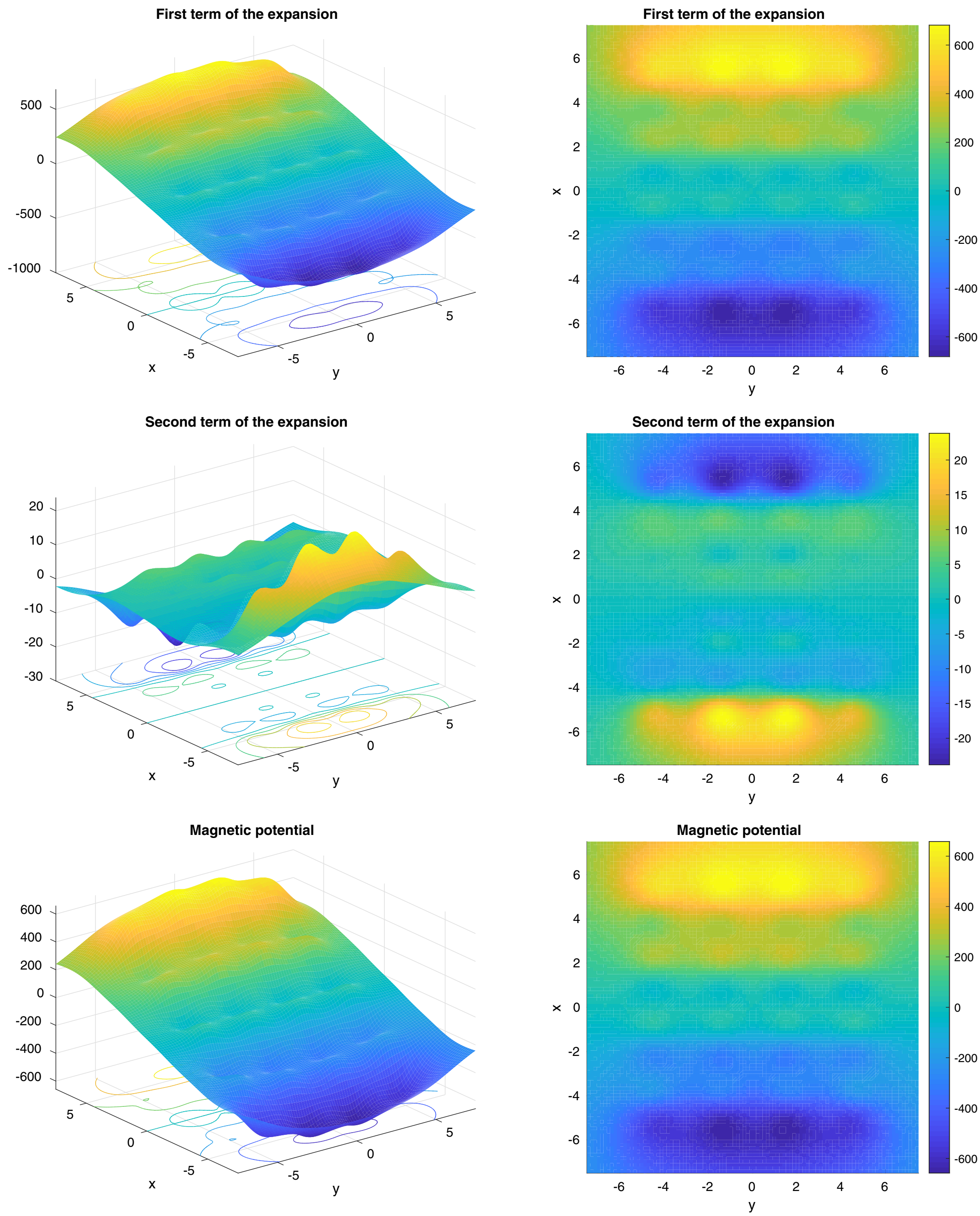

FIGURE 9. Cube of 64 equidistant particles. *From top to bottom*: First term in the series expansion of the magnetic potential, second term in the series expansion and approximation of the magnetic potential obtained by summing the first two terms of the series expansion. *From left to right*: Three-dimensional shaded surface representation and two-dimensional representation of the three quantities.

$x \in \mathbb{R}^3$. Moreover, the series expansion (5.1) can be interpreted as a discrete spherical Fourier transform and fast spherical Fourier algorithms can be used for a fast evaluation of the finite sum. Given D computational nodes arbitrary spaced on the sphere, the computational complexity of a fast spherical Fourier algorithms is $\mathcal{O}(L^2 \log^2(L)+p^2 D)$ where p is a cut off parameter [16]. Therefore, the computational complexity of the pairwise interactions method would be $\mathcal{O}\big(N^2(L^2 \log^2(L)+p^2 D)\big)$. Note that various optimizations as described *e.g.* in [26] can be used to fasten the computations and that a very interesting feature of the method is that it is easily parallelizable: Each pair of particles can be handle separately.

A limitation of the method is that it is not designed to deal with distributions of nearly touching particles. Taking into account pairwise interactions greatly improves the accuracy of magnetic field computations compared to the non-interaction assumption when the particles are close to each other but for nearly touching particles higher order interactions need to be taken into account.

6. Conclusion

In the first part of the paper, we have investigated the validity of the approach consisting in neglecting magnetic interactions between particles in the numerical computation of the magnetic field inhomogeneities induced by a cluster of metallic particles subjected to a uniform magnetic field. Such a situation is encountered in various contexts in Magnetic Resonance Imaging. We have obtained bounds for the approximation error in terms of the three geometrical key parameters that were found to be the number of particles N, the radius ε of the particles (assumed to have a spherical shape for simplicity), and the distance δ between the two nearest particles. Two other physical parameters, the magnetic permeability μ_p of the particles and the strength of the inductive magnetic field H_0 are also involved in the error bound. The main conclusion of the analysis carried out on the “non-interacting assumption” is that the error is proportional to ε^4/δ^3. This behavior has also been observed in numerical experiments presented in the paper.

When the “non-interacting assumption” is deficient, we have proposed in the second part of the paper a method to compute a better approximation of the magnetic potential by taking into account pairwise magnetic field interactions between particles. Numerical computation of pairwise magnetic field interactions relies on the evaluation of spherical harmonics series by fast spherical Fourier algorithms. The method has good parallelisation properties which suggests that an efficient simulation software could be developed to deal with *e.g.* the applications in MRI quoted in the introduction. We have also obtained error bounds in terms of the above mentioned key parameters for the approximation of the magnetic potential taking into account pairwise interactions.

Appendix A. Trace and injection

It is well known (*e.g.* [6], p. 119) that functions belonging to $\mathbb{W}^1_0(\mathbb{R}^3)$ admit a trace on the surfaces Σ_j, $j \in \{1,\dots,N\}$, and that the trace defines a continuous mapping from $\mathbb{W}^1_0(\mathbb{R}^3)$ onto $\mathbb{H}^{\frac12}(\Sigma_j)$. From Sobolev's embedding results, we also deduce that $\mathbb{W}^1_0(\mathbb{R}^3)$ is continuously injected in $\mathbb{L}^1(\Sigma_j)$:

$$\forall j \in \{1,\dots,N\} \quad \exists C_j > 0 \quad \forall \varphi \in \mathbb{W}^1_0(\mathbb{R}^3) \quad \|\varphi\|_{\mathbb{L}^1(\Sigma_j)} \leqslant C_j \|\varphi\|_{\mathbb{W}^1(\mathbb{R}^3)}.$$

The following proposition set out the constants C_j when the surfaces Σ_j are spheres with radius ε.

Proposition A.1. *For all $j \in \{1,\dots,N\}$ and for all $\varphi \in \mathbb{W}^1_0(\mathbb{R}^3)$*

$$\|\varphi\|_{\mathbb{L}^1(\Sigma_j)} \leqslant A_1\, \varepsilon^{\frac32}\, \|\varphi\|_{\mathbb{W}^1(\mathbb{R}^3)} \tag{A.1}$$

where $A_1 = \sqrt{4\pi}$.

Proof. We first consider the case where Σ_j is the unit sphere S^2 centered at the origin and with radius 1. By a density argument, we can consider functions ψ in $\mathcal{C}_0^\infty(\mathbb{R}^3)$. In the spherical coordinates system (r,θ,η), we have

$$\int_{S^2} |\psi(1,\theta,\eta)| \sin\theta \,\mathrm{d}\theta\,\mathrm{d}\eta \leqslant \int_1^\infty \int_{S^2} |\partial_r\psi(r,\theta,\eta)| \sin\theta \,\mathrm{d}\theta\,\mathrm{d}\eta\,\mathrm{d}r$$
$$\leqslant \sqrt{\int_1^\infty \int_{S^2} \frac{1}{r^2} \sin\theta \,\mathrm{d}\theta\,\mathrm{d}\eta\,\mathrm{d}r}\sqrt{\int_1^\infty \int_{S^2} |\partial_r\psi(r,\theta,\eta)|^2 r^2 \sin\theta \,\mathrm{d}\theta\,\mathrm{d}\eta\,\mathrm{d}r}.$$

It follows that

$$\|\psi\|_{\mathbb{L}^1(S)} \leqslant \sqrt{4\pi}\, \|\psi\|_{\mathbb{W}^1(\mathbb{R}^3)}. \tag{A.2}$$

In the case where Σ_j is a sphere centered in c_j with radius $\varepsilon > 0$, we use the change of variable $y \in S^2 \mapsto x = c_j + \varepsilon y \in \Sigma_j$. More precisely, for $\varphi \in \mathbb{W}_0^1(\mathbb{R}^3)$ we define ψ such that $\psi(y) = \varphi(x)$. We have

$$\|\varphi\|_{\mathbb{L}^1(\Sigma_j)} = \varepsilon^2 \|\psi\|_{\mathbb{L}^1(S)} \quad \text{and} \quad \|\varphi\|_{\mathbb{W}^1(\mathbb{R}^3)} = \sqrt{\varepsilon}\|\psi\|_{\mathbb{W}^1(\mathbb{R}^3)}. \tag{A.3}$$

Estimate (A.2) together with (A.3) directly imply (A.1). □

The Sobolev injection indicates that $\mathbb{H}^{\frac{1}{2}}(\Sigma_j) \subset \mathbb{L}^4(\Sigma_j)$ and we also have the following finer result.

Proposition A.2. *For all $j \in \{1,\dots,N\}$ and for all $\varphi \in \mathbb{W}_0^1(\mathbb{R}^3)$*

$$\|\varphi\|_{\mathbb{L}^4(\Sigma_j)} \leqslant A_2 \|\varphi\|_{\mathbb{W}^1(\mathbb{R}^3)} \tag{A.4}$$

where $A_2 = \frac{2}{3^{\frac{3}{8}}\sqrt{\pi}}$.

Proof. As in the proof of Proposition A.1, we only have to deal with the case where Σ_j is the unit sphere S^2. We also assume that φ belongs to $\mathcal{C}_0^\infty(\mathbb{R}^3)$ since the estimate for $\varphi \in \mathbb{W}_0^1(\mathbb{R}^3)$ will follow by density. Using the spherical coordinates (r,θ,η), we have

$$\|\varphi\|^4_{\mathbb{L}^4(S^2)} = \int_{S^2} |\varphi(1,\theta,\eta)|^4 \sin\theta \,\mathrm{d}\theta\,\mathrm{d}\eta \leqslant 4\int_1^\infty\int_{S^2} |\varphi(r,\theta,\eta)|^3 |\partial_r\varphi(r,\theta,\eta)| \sin\theta \,\mathrm{d}\theta\,\mathrm{d}\eta\,\mathrm{d}r$$
$$\leqslant 4\sqrt{\int_1^\infty\int_{S^2} |\varphi(r,\theta,\eta)|^6 \sin\theta \,\mathrm{d}\theta\,\mathrm{d}\eta\,\mathrm{d}r}\sqrt{\int_1^\infty\int_{S^2} |\partial_r\varphi(r,\theta,\eta)|^2 \sin\theta \,\mathrm{d}\theta\,\mathrm{d}\eta\,\mathrm{d}r}$$
$$\leqslant 4\|\varphi\|^3_{\mathbb{L}^6(\mathbb{R}^3)} \|\varphi\|_{\mathbb{W}^1(\mathbb{R}^3)}.$$

Using the following Sobolev embedding result in $\mathbb{R}^3$, see [8], p. 26,

$$\|\varphi\|^3_{\mathbb{L}^6(\mathbb{R}^3)} \leqslant \left(\frac{4}{3}\right)^{\frac{3}{2}} \frac{1}{2\pi^2} \|\nabla\varphi\|^3_{\mathbb{L}^2(\mathbb{R}^3)}. \tag{A.5}$$

we deduce that $\|\varphi\|_{\mathbb{L}^4(S^2)} \leqslant \frac{2}{3^{\frac{3}{8}}\sqrt{\pi}} \|\varphi\|_{\mathbb{W}^1(\mathbb{R}^3)}$. □

Appendix B. Some results on the sum of powers of the inverse distance

Proposition B.1. *Let $\Omega_1,\dots,\Omega_N$ be N spherical particles in $B(0,1) \subset \mathbb{R}^3$, centered respectively at c_j, $j \in \{1,\dots,N\}$, with the same radius $\varepsilon > 0$. Let δ be the minimal distance between two particles as defined in (1.1). For all $i \in \{1,\dots,N\}$ and for all $x \in \mathbb{R}^3$ such that* $\operatorname{dist}(x,\Sigma_i) \leqslant \frac{\delta}{2}$, *we have*

$$\sum_{\substack{j=1\\ j\neq i}}^N \frac{1}{|c_j - x|^3} \leqslant \left(B_3 + 3\ln\left(\frac{2}{\delta}\right)\right)\left(\frac{2}{\delta}\right)^3 \tag{B.1}$$

where $B_3 = 142 + 3\ln 2 \approx 144.1$. *Moreover, for all* $p \geqslant 4$, *we have*

$$\sum_{\substack{j=1\\ j\neq i}}^{N} \frac{1}{|c_j - x|^p} \leqslant 137 \left(\frac{2}{\delta}\right)^p. \tag{B.2}$$

Proof. Let $i \in \{1, \dots, N\}$, $x \in \mathbb{R}^3$ such that $\mathrm{dist}(x, \Sigma_i) \leqslant \frac{\delta}{2}$. For $p \geqslant 1$, we split the sum

$$S_i^{(p)}(x) = \sum_{\substack{j=1\\ j\neq i}}^{N} \frac{1}{|c_j - x|^p}$$

into two parts. The first one concerns the indices j such that the particles Ω_j with center c_j are at a distance lower than 2δ from Ω_i. The second one concerns the indices j such that the particles Ω_j are not in this neighborhood. Moreover, since the volume of the ball $B(c_j, \frac{\delta}{2})$ is $\frac{\pi}{6}\delta^3$, we have

$$S_i^{(p)}(x) = \sum_{\substack{j=1,\ j\neq i\\ |c_j - c_i| < 2\delta}}^{N} \frac{1}{|c_j - x|^p} + \sum_{\substack{j=1,\ j\neq i\\ |c_j - c_i| \geqslant 2\delta}}^{N} \frac{6}{\pi\delta^3} \int_{B(c_j, \frac{\delta}{2})} \frac{\mathrm{d}y}{|c_j - x|^p}. \tag{B.3}$$

The number of terms in the first sum in the RHS of (B.3), denoted $S_{i,1}^{(p)}$ in the sequel, is bounded independently of N. Actually, this number is lower than the cardinal number C of the set of points in $B(0,2) \setminus B(0,1)$, such that the pairwise distance is larger than 1. By volume considerations, this number is found to be less than the quotient obtained by dividing the volume of $B(0, \frac{5}{2}) \setminus B(0, \frac{1}{2})$ by the volume of $B(0, \frac{1}{2})$ that is to say 124. Each term in $S_{i,1}$ is smaller than $\frac{1}{(\delta/2)^p}$ so that

$$S_{i,1}^{(p)} \leqslant 124 \left(\frac{2}{\delta}\right)^p. \tag{B.4}$$

Let us now obtain an estimate of the second sum in the RHS of (B.3), denoted $S_{i,2}^{(p)}$ in the sequel. First of all, from the triangular inequality, we note that for all $y \in B(c_j, \frac{\delta}{2})$,

$$|y - c_i| \leqslant |y - c_j| + |c_j - x| + |x - c_i| \leqslant \frac{\delta}{2} + |x - c_j| + \frac{\delta}{2} = |x - c_j| + \delta.$$

It follows that $|x - c_j| \geqslant |y - c_i| - \delta$ and

$$S_{i,2}^{(p)} \leqslant \frac{6}{\pi\,\delta^3} \sum_{\substack{j=1,\ j\neq i\\ |c_j - c_i| \geqslant 2\delta}}^{N} \int_{B(c_j, \frac{\delta}{2})} \frac{\mathrm{d}y}{(|y - c_i| - \delta)^p} \leqslant \frac{6}{\pi\,\delta^3} \int_{B(c_i, 2)\setminus B(c_i, \frac{3}{2}\delta)} \frac{\mathrm{d}y}{(|y - c_i| - \delta)^p} \tag{B.5}$$

since under our assumptions for all $j \in \{1, \dots, N\}$, $j \neq i$, we have $B(c_j, \frac{\delta}{2}) \subset B(c_i, 2) \setminus B(c_i, \frac{3}{2}\delta)$. The last integral in (B.5) can be expressed in spherical coordinates, and then it can be explicitly evaluated. We obtain

$$S_{i,2}^{(p)} \leqslant \frac{24}{\delta^3} \int_{\frac{3}{2}\delta}^{2} \frac{r^2\,\mathrm{d}r}{(r - \delta)^p} = \frac{24}{\delta^3} \int_{\frac{\delta}{2}}^{2-\delta} \frac{(s + \delta)^2}{s^p}\,\mathrm{d}s := \frac{24}{\delta^3}\, I_p.$$

We now distinguish the different possible values of p envisaged in the proposition since the integral takes different closed form expressions depending on the value of p.

– Case $p = 3$. We have

$$I_3 = \int_{\frac{\delta}{2}}^{2-\delta} \frac{(s+\delta)^2}{s^3}\, \mathrm{d}s = \frac{48 - 56\delta + 15\delta^2}{2(2-\delta)^2} + \ln\left(\frac{2}{\delta}(2-\delta)\right).$$

From (B.3) and (B.4), we deduce that

$$S_i^{(3)} \leqslant (3I_3 + 124)\, \left(\frac{2}{\delta}\right)^3.$$

One can show that the mapping $\delta \mapsto I_2$ is bounded by $18 + \ln 2 + \ln\left(\frac{2}{\delta}\right)$. This conclude the proof of (B.1).

– Case $p \geqslant 4$. We have

$$I_p = \int_{\frac{\delta}{2}}^{2-\delta} \frac{(s+\delta)^2}{s^p}\, \mathrm{d}s = \left[\frac{s^{3-p}}{3-p} + \frac{2\delta s^{2-p}}{2-p} + \frac{\delta^2 s^{1-p}}{1-p}\right]_{\frac{\delta}{2}}^{2-\delta} \leqslant \frac{13}{3}\left(\frac{2}{\delta}\right)^{p-3}.$$

We deduce that

$$S_{i,2}^{(p)} \leqslant 13\left(\frac{2}{\delta}\right)^p.$$

From (B.3) and (B.4), we deduce the estimate (B.2).

□

One of the important feature of the estimates given in proposition (B.1) is that they are optimal. More precisely, the behaviour of the sums with respect to the variable δ is correctly estimated. This remark can be understood by looking at the case of a large number of particles ($N \to +\infty$) uniformly distributed in the ball $B(0,1)$, with one particle located at the origin. To illustrate the situation, we consider the case $p = 3$. Let assume that $c_1 = (0,0,0)$ for simplicity. Since δ measures the distance between the centers of two "adjacent" particles, these centers have for coordinates $(k_1\delta, k_2\delta, k_3\delta)$ where $(k_1,k_2,k_3) \in \mathbb{Z}^3$ with $\delta^2(k_1^2+k_2^2+k_3^2) \leqslant 1$. It is clear that the "worst" case, i.e. the one that makes the largest the sum $S_i^{(3)}$, is the case $i = 1$. Thus, let us consider $S_1^{(3)}(0)$. For all $j \in \{2,\ldots,N\}$, we have

$$S_1^{(3)}(0) = \sum_{\substack{j=1\\ j\neq 1}}^{N} \frac{1}{|c_j|^3} = \sum_{\substack{(k_1,k_2,k_3)\in\mathbb{Z}^3\\ 1\leqslant k_1^2+k_2^2+k_3^2 \leqslant \frac{1}{\delta^2}}} \frac{1}{(\delta\sqrt{k_1^2+k_2^2+k_3^2})^3} = \frac{1}{\delta^3}\sum_{\substack{(k_1,k_2,k_3)\in\mathbb{Z}^3\\ 1\leqslant k_1^2+k_2^2+k_3^2 \leqslant \frac{1}{\delta^2}}} \frac{1}{(k_1^2+k_2^2+k_3^2)^{\frac{3}{2}}}\cdot$$

When N is large, the last sum is the approximation by the mid-ordinate quadrature rule of the integral

$$I = \frac{1}{\delta^3}\int_{B(0,\frac{1}{\delta})\setminus B(0,1)} \frac{\mathrm{d}x}{(x_1^2+x_2^2+x_3^2)^{\frac{3}{2}}}\cdot$$

This integral can be easily evaluated using spherical coordinates and we obtain

$$I = \frac{4\pi}{\delta^3}\int_1^{\frac{1}{\delta}} \frac{\mathrm{d}r}{r} = \frac{4\,\pi}{\delta^3}\ln\left(\frac{1}{\delta}\right)\cdot \tag{B.6}$$

This shows that the estimate given in proposition B.1 in the case $p = 3$ is optimal in the following sense: for $\delta = o(1)$ (that precisely corresponds to the case of many particles uniformly distributed in the ball $B(0,1)$), estimate (B.1) reads

$$S_1^{(3)}(0) \leqslant \frac{a}{\delta^3}\,\ln\left(\frac{1}{\delta}\right),$$

the constant a being independent of N, δ and ε, whereas in the present example, using (B.6), we have

$$S_1^{(3)}(0) \geqslant \frac{b}{\delta^3}\,\ln\left(\frac{1}{\delta}\right),$$

where b is another constant independent of N, δ and ε.

Appendix C. Some results on the Spherical Surface Harmonics

Proposition C.1. *For $\ell \in \mathbb{N}$, the family of spherical harmonics $(Y_\ell^m)_{-\ell\leqslant m\leqslant \ell}$ satisfies:*

$$\forall(\theta,\eta)\in[0,\pi]\times[0,2\pi] \qquad \sum_{m=-\ell}^{\ell}|Y_\ell^m(\theta,\eta)| \leqslant \frac{3\sqrt{3}}{\sqrt{4\pi}}\,\ell^{\frac{3}{2}}. \tag{C.1}$$

Proof. From the definition of Spherical Surface Harmonics, we have

$$\sum_{m=-\ell}^{\ell}|Y_\ell^m(\theta,\eta)| = \sqrt{\frac{2\ell+1}{4\pi}}\left(|P_\ell^0(\cos(\theta))| + 2\sum_{m=1}^{\ell}\sqrt{\frac{(\ell-m)!}{(\ell+m)!}}\,|P_\ell^m(\cos(\theta))|\right).$$

The Legendre polynomial $P_\ell^0 = P_\ell$ is bounded by 1 and we have the following bounds for the Associated Legendre functions, see [19],

$$\forall m\in\{1,\dots,\ell\} \qquad \sqrt{\frac{(\ell-m)!}{(\ell+m)!}}\max_{x\in[-1,1]}|P_\ell^m(x)| \leqslant \frac{1}{\sqrt{2}}\cdot \tag{C.2}$$

It follows that

$$\sum_{m=-\ell}^{\ell}|Y_\ell^m(\theta,\eta)| \leqslant \sqrt{\frac{2\ell+1}{4\pi}}(1+\sqrt{2}\ell) \leqslant \frac{(2\ell+1)^{\frac{3}{2}}}{\sqrt{4\pi}} \leqslant \frac{3\sqrt{3}}{\sqrt{4\pi}}\,\ell^{\frac{3}{2}}.$$

□

Proposition C.2. *For $\ell \in \mathbb{N}$, the family of spherical harmonics $(Y_\ell^m)_{-\ell\leqslant m\leqslant \ell}$ satisfies:*

$$\forall(\theta,\eta)\in[0,\pi]\times[0,2\pi] \qquad \sum_{m=-\ell}^{\ell}|\partial_\theta Y_\ell^m(\theta,\eta)| \leqslant \frac{\sqrt{3}(1+\pi)}{\sqrt{2\pi}}\,\ell^{\frac{5}{2}}. \tag{C.3}$$

Proof. Using the definition of the Spherical Harmonics, we get

$$\sum_{m=-\ell}^{\ell}|\partial_\theta Y_\ell^m(\theta,\eta)| \leqslant \sqrt{\frac{2\ell+1}{4\pi}}\left(|\partial_\theta P_\ell^0(\cos(\theta))| + 2\sum_{m=1}^{\ell}\sqrt{\frac{(\ell-m)!}{(\ell+m)!}}\,|\partial_\theta P_\ell^m(\cos(\theta))|\right).$$

For all $\ell\geqslant 1$, for all $m\in\{1,\dots,\ell\}$ and for all $x\in]-1,1[$, we have [1, 20]:

$$\begin{aligned}
\partial_x P_\ell^0(x) &= \partial_x P_\ell(x) = -\frac{1}{\sqrt{1-x^2}}\,P_\ell^1(x)\\
\partial_x P_\ell^m(x) &= \frac{1}{2\sqrt{1-x^2}}\Big((\ell+m)(\ell-m+1)\,P_\ell^{m-1}(x) - P_\ell^{m+1}(x)\Big).
\end{aligned}$$

It follows that for all $\ell\geqslant 1$, for all $m\in\{1,\dots,\ell\}$ and for all $\theta\in[0,\pi]$

$$\begin{aligned}
\partial_\theta P_\ell^0(\cos(\theta)) &= P_\ell^1(\cos(\theta))\\
\partial_\theta P_\ell^m(\cos(\theta)) &= \frac{1}{2}\Big(P_\ell^{m+1}(\cos(\theta)) - (\ell+m)(\ell-m+1)\,P_\ell^{m-1}(\cos(\theta))\Big).
\end{aligned}$$

Using relations (C.2) we deduce that

$$\begin{aligned}
\sum_{m=-\ell}^{\ell}|\partial_\theta Y_\ell^m(\theta,\eta)| &\leqslant \sqrt{\frac{2\ell+1}{8\pi}}\sum_{m=-\ell}^{\ell}\sqrt{(\ell+m)(\ell+1-m)}\\
&\leqslant \sqrt{\frac{2\ell+1}{8\pi}}\sum_{m=-\ell}^{\ell}\sqrt{(\ell+1)^2-m^2}.
\end{aligned}$$

By comparison to the quadrature rectangle rule, we have

$$\begin{aligned}\sum_{m=-\ell}^{\ell} \sqrt{(\ell+1)^2-m^2} &= (\ell+1) + 2\sum_{m=1}^{\ell} \sqrt{(\ell+1)^2-m^2}\\ &\leqslant (\ell+1) + 2\int_0^{\ell+1} \sqrt{(\ell+1)^2-x^2}\ \mathrm{d}x\\ &\leqslant (\ell+1) + \frac{\pi}{2}(\ell+1)^2.\end{aligned}$$

To conclude the proof, note that $2\ell+1 \leqslant 3\ell$ and $(\ell+1)+\frac{\pi}{2}(\ell+1)^2 \leqslant 2(1+\pi)\ell^2$. □

Proposition C.3. *For $\ell \in \mathbb{N}$, the family of spherical harmonics $(Y_\ell^m)_{-\ell\leqslant m\leqslant \ell}$ satisfies:*

$$\forall(\theta,\eta) \in [0,\pi]\times[0,2\pi] \qquad \sum_{m=-\ell}^{\ell} \left|\frac{1}{\sin(\theta)}\partial_\eta Y_\ell^m(\theta,\eta)\right| \leqslant \frac{3\sqrt{3}}{2\sqrt{2\pi}}\,\ell^{\frac{5}{2}}. \tag{C.4}$$

Proof. Using the definition of the Spherical Harmonics, we express the sum in the LHS of (C.4) using the associated Legendre polynomials as

$$\sum_{m=-\ell}^{\ell} \left|\frac{1}{\sin(\theta)}\partial_\eta Y_\ell^m(\theta,\eta)\right| = \sqrt{\frac{2\ell+1}{4\pi}} \sum_{m=-\ell}^{\ell} \sqrt{\frac{(\ell-m)!}{(\ell+m)!}} \left|\frac{m}{\sin(\theta)} P_\ell^m(\cos(\theta))\right|. \tag{C.5}$$

For all $\ell \geqslant 1$, for all $m \in \{1,\ldots,\ell\}$ and for all $x \in]-1,1[$, we have [1,20]:

$$\frac{m}{2\sqrt{1-x^2}}\,P_\ell^m(x) = -P_{\ell-1}^{m+1}(x) - (\ell+m)(\ell+m-1)\,P_{\ell-1}^{m-1}(x).$$

It follows that for all $\ell \geqslant 1$, for all $m \in \{1,\ldots,\ell\}$ and for all $\theta \in [0,\pi]$

$$\frac{m}{2\sin(\theta)}\,P_\ell^m(\cos(\theta)) = -P_{\ell-1}^{m+1}(\cos(\theta)) - (\ell+m)(\ell+m-1)\,P_{\ell-1}^{m-1}(\cos(\theta)).$$

Following the same steps as in the proof of Proposition C.2, we conclude that

$$\begin{aligned}\sum_{m=-\ell}^{\ell} \left|\frac{1}{\sin(\theta)}\partial_\eta Y_\ell^m(\theta,\eta)\right| &\leqslant \frac{\sqrt{2\ell+1}}{2\sqrt{2\pi}} \sum_{m=-\ell}^{\ell} \sqrt{(\ell-m)(\ell-m-1)}\\ &\leqslant \frac{\sqrt{2\ell+1}}{2\sqrt{2\pi}} \sum_{m=-\ell}^{\ell} (\ell-m) \leqslant \frac{\ell(2\ell+1)^{\frac{3}{2}}}{2\sqrt{2\pi}} \leqslant \frac{3\sqrt{3}}{2\sqrt{2\pi}}\,\ell^{\frac{5}{2}}.\end{aligned}$$

□

Appendix D. L^p-norm of the normal derivative of Green's kernel

Proposition D.1. *For all $x \in \mathbb{R}^3$, we have*

$$\|\partial_n \mathcal{G}(x,\cdot)\|_{\mathbb{L}^{\frac{4}{3}}(S^2)} \leqslant A_3 \tag{D.1}$$

where $A_3 = \|\partial_n \mathcal{G}((1,0,0),\cdot)\|_{\mathbb{L}^{\frac{4}{3}}(S^2)} \approx 0.3439.$

Proof. We proceed in two steps. First, we will compute the expression of $\|\partial_n \mathcal{G}(x^\star, \cdot)\|_{\mathbb{L}^{\frac{4}{3}}(S^2)}$ for all $x^\star \in S^2$. Then we will show that for all $x \in \mathbb{R}^3$, denoting by $x^\star \in S^2$ the projection of x onto S^2, we have

$$\forall y \in S^2 \setminus \{x^\star\} \qquad |\partial_n \mathcal{G}(x, y)| \leqslant |\partial_n \mathcal{G}(x^\star, y)|. \tag{D.2}$$

For all $x^\star \in S^2$ and for all p such that $1 < p < 2$, let us consider the quantity

$$\mathcal{A} = \oint_{S^2} \left| \frac{n \cdot (x^\star - y)}{4\pi |x^\star - y|^3} \right|^p \, \mathrm{d}y$$

where n denotes the outward unit normal to S^2 at $y \in S^2$. In order to compute $\mathcal{A}$, let us consider a frame centered on $x^\star$ and the following parametrization of the unit sphere S^2:

$$(s, t) \in B(0, 1) \subset \mathbb{R}^2 \longmapsto \begin{pmatrix} s \\ t \\ 1 \pm \sqrt{1 - s^2 - t^2} \end{pmatrix} \in S^2$$

where the sign $\pm$ is introduced to describe the two hemispheres and $B(0, 1)$ denotes the unit ball in $\mathbb{R}^2$. In this frame, the normal unit vector n to the sphere S^2 is given by $n = \left(s,\, t,\, \pm\sqrt{1 - s^2 - t^2}\right)^\top$. Since $|y|^2 = 2n \cdot y$, we have $\mathcal{A} = \mathcal{A}_+ + \mathcal{A}_-$ where

$$\mathcal{A}_\pm = \frac{1}{(8\pi)^p} \iint_{s^2+t^2<1} \frac{1}{(2 \pm 2\sqrt{1 - s^2 - t^2})^{\frac{p}{2}}} \frac{\sqrt{1 + s^2 + t^2}}{\sqrt{1 - s^2 - t^2}} \, \mathrm{d}s \, \mathrm{d}t = \frac{1}{2^{\frac{7p}{2}-1} \pi^{p-1}} \int_0^1 \frac{1}{(1 \pm \sqrt{1 - r^2})^{\frac{p}{2}}} \frac{\sqrt{1 + r^2}}{\sqrt{1 - r^2}} \, r \, \mathrm{d}r.$$

Using the change of variable $u = 1 \pm \sqrt{1 - r^2}$, we deduce that

$$\mathcal{A} = \frac{1}{2^{\frac{7p}{2}-1} \pi^{p-1}} \int_0^2 \frac{\sqrt{1 + 2u - u^2}}{u^{\frac{p}{2}}} \, \mathrm{d}u.$$

For $p = \frac{4}{3}$, by evaluating $\mathcal{A}$ by quadrature, we find $\mathcal{A} \approx 0.24093027$. Finally,

$$\|\partial_n \mathcal{G}(x^\star, \cdot)\|_{\mathbb{L}^{\frac{4}{3}}(S^2)} = \mathcal{A}^{\frac{3}{4}} \leqslant 0.35. \tag{D.3}$$

In order to prove (D.1), we consider $x \in \mathbb{R}^3$ and we denote by $x^\star$ its projection onto S^2. Considering the frame previously introduced and centered on $x^\star$. The coordinate of x are $(0, 0, -d)$ where $d = \operatorname{dist}(x, S^2) \geqslant 0$. For any point $y \in S^2$, we deduce from the relation $|y|^2 = 2n \cdot y$ that

$$\left| \frac{n \cdot (x^\star - y)}{|x^\star - y|^3} \right| = \frac{1}{2|y|}.$$

Similarly, one can show that

$$\left| \frac{n \cdot (x - y)}{|x - y|^3} \right| = \frac{1}{2|x - y|} - \frac{d^2 + 2d}{2|x - y|^3}.$$

Since $d \geqslant 0$ and $|x - y| \geqslant |x^\star - y|$, we directly deduce that

$$\left| \frac{n \cdot (x - y)}{|x - y|^3} \right| \leqslant \left| \frac{n \cdot (x^\star - y)}{|x^\star - y|^3} \right|.$$

This last inequality implies that $\|\partial_n \mathcal{G}(x, \cdot)\|_{\mathbb{L}^{\frac{4}{3}}(S^2)} \leqslant \|\partial_n \mathcal{G}(x^\star, \cdot)\|_{\mathbb{L}^{\frac{4}{3}}(S^2)}$. We conclude the proof of Proposition D.1 using relation (D.3). $\square$

Appendix E. Constants introduced in this study

Table E.1. Values of the constants introduced in the study.

Name	Defined in ...	Exact value	Approximate value
A_1	Proposition A.1	$\sqrt{4\pi}$	$3.5 \times 10^{+0}$
A_2	Proposition A.2	$2/(3^{\frac{3}{8}}\sqrt{\pi})$	7.5×10^{-1}
A_3	Proposition D.1	$\Vert\partial_n \mathcal{G}((1,0,0),\cdot)\Vert_{\mathbb{L}^{\frac{4}{3}}(S^2)}$	3.5×10^{-1}
A_4	Proposition 4.4	$2\sqrt{6(85+8\pi+4\pi^2)}$	$6.0 \times 10^{+1}$
B_1	Lemma 3.5	$\frac{3}{4}\max\limits_{\delta>0}\left(8+8\delta-6\delta^2+\delta^2\ln\left(\frac{2}{\delta}\right)\right)$	$8.4 \times 10^{+0}$
B_2	Lemma 3.5	$\frac{\sqrt{2}}{3\,\pi^{\frac{1}{4}}}\max\limits_{\delta>0}\left(8-6\delta-\delta^2+8\delta\ln\left(\frac{2}{\delta}\right)\right)$	$6.6 \times 10^{+0}$
B_3	Proposition B.1	$124+3\ln 2$	$1.4 \times 10^{+2}$

References

[1] M. Abramowitz and I.A. Stegun, Handbook of Mathematical Functions: With Formulas, Graphs, and Mathematical Tables. *Dover Books on Mathematics*. Dover Publications (1965).

[2] S. Balac and G. Caloz, Mathematical modeling and numerical simulation of magnetic susceptibility artifacts in Magnetic Resonance Imaging. *Comput. Methods Biomech. Biomed. Eng.* **3** (2000) 335–349.

[3] J.L. Boxerman, L.M. Hamberg, B.R. Rosen and R.M. Weisskoff, MR contrast due to intravascular magnetic susceptibility perturbations. *Magn. Reson. Med.* **34** (1995) 555–566.

[4] H. Cheng, On the method of images for systems of closely spaced conducting spheres. *SIAM J. Appl. Math.* **61** (2001) 1324–1337.

[5] J.-Y. Chung, Y.-W. Sung and S. Ogawa, Evaluation of the contribution of signals originating from large blood vessels to signals of functionally specific brain areas. *BioMed Res. Int.* **2015** (2015) 234345.

[6] R. Dautray and J.L. Lions, Analyse mathématique et calcul numérique pour les sciences et les techniques. Vol. 4 of Collection Enseignement – INSTN CEA. Masson (1988).

[7] J. Deny and J.L. Lions, Les espaces du type de Beppo Levi. *Ann. Inst. Fourier* **5** (1954) 305–370.

[8] O. Druet, Inégalités de Sobolev optimales et inégalités isopérimétriques sur les variétés. *Séminaire de théorie spectrale et géométrie* **20** (2001–2002) 23–100.

[9] S. Fujiwara, L. Uhrig, A. Amadon, B. Jarraya and D. Le Bihan, Quantification of iron in the non-human primate brain with diffusion-weighted magnetic resonance imaging. *NeuroImage* **102** (2014) 789–797.

[10] Z. Gan, S. Jiang, E. Luijten and Z. Xu, A hybrid method for systems of closely spaced dielectric spheres and ions. *SIAM J. Sci. Comput.* **38** (2016) B375–B395.

[11] F. Hecht, New development in FreeFem++. *J. Numer. Math.* **20** (2012) 251–265.

[12] J. Jin, The Finite Element Method in Electromagnetics, 3rd edition. Wiley-IEEE Press (2014).

[13] S.-G. Kim, N. Harel, T. Jin, T. Kim, P. Lee and F. Zhao, Cerebral blood volume MRI with intravascular superparamagentic iron oxide nanoparticles. *NMR in Biomed.* **26** (2013) 949–962.

[14] V.G. Kiselev, Effect of magnetic field gradients induced by microvasculature on NMR measurements of molecular self-diffusion in biological tissues. *J. Magn. Reson.* **170** (2004) 228–235.

[15] V. Kiselev and S. Posse, Analytical model of susceptibility-induced MR signal dephasing: Effect of diffusion in a microvascular network. *Magn. Reson. Med.* **41** (1999) 499–509.

[16] S. Kunis and D. Potts, Fast spherical Fourier algorithms. *J. Comput. Appl. Math.* **161** (2003) 75–98.

[17] K.S. Kunz and R.J. Luebbers, The Finite Difference Time Domain Method for Electromagnetics. CRC Press (1993).

[18] E.B. Lindgren, A.J. Stace, E. Polack, Y. Maday, B. Stamm and E. Besley, An integral equation approach to calculate electrostatic interactions in many-body dielectric systems. *J. Comput. Phys.* **371** (2018) 712–731.

[19] G. Lohöfer, Inequalities for the associated Legendre functions. *J. Approximation Theory* **95** (1998) 178–193.

[20] F.W.J. Olver, D.W. Lozier, R.F. Boisvert and C.W. Clark, NIST Handbook of Mathematical Functions. Cambridge University Press (2010).

[21] A.P. Pathak, B.D. Ward and K.M. Schmainda, A novel technique for modeling susceptibility-based contrast mechanisms for arbitrary microvascular geometries: The finite perturber method. *NeuroImage* **40** (2008) 1130–1143.

[22] J. Qin, J.J. de Pablo and K.F. Freed, Image method for induced surface charge from many-body system of dielectric spheres. *J. Chem. Phys.* **145** (2016) 124903.

[23] W.J. Rogers, C.H. Meyer and C.M. Kramer, Technology insight: in vivo cell tracking by use of MRI. *Nat. Clin. Pract. Cardiovasc. Med.* **3** (2006) 554–562.

[24] V. Rokhlin and M. Tygert, Fast algorithms for spherical harmonic expansions. *SIAM J. Sci. Comput.* **27** (2006) 1903–1928.

[25] G. Sansone, Orthogonal functions. *Dover Books on Mathematics Series*. Dover Publications (2004).

[26] N. Schaeffer, Efficient spherical harmonic transforms aimed at pseudospectral numerical simulations. *Geochem. Geophys. Geosyst.* **14** (2013) 751–758.

[27] J.F. Schenck, The role of magnetic susceptibility in Magnetic Resonance Imaging: MRI magnetic compatibility of the first and second kinds. *Med. Phys.* **23** (1996) 815–850.

[28] J.L. Volakis and S. Sertel, Integral equation methods for electromagnetics. In: Electromagnetic Waves. Institution of Engineering and Technology (2012).

[29] C. Weis, F. Blank, A. West, G. Black, R.C. Woodward, M.R. Carroll, A. Mainka, R. Kartmann, A. Brandl, H. Bruns and E. Hallam, Labeling of cancer cells with magnetic nanoparticles for MRI. *Magn. Reson. Med.* **71** (2014) 1896–1905.

[30] D.A. Yablonskiy and E.M. Haacke, Theory of NMR signal behavior in magnetically inhomogeneous tissues: The static dephasing regime. *Magn. Reson. Med.* **32** (1994) 749–763.

[31] L. Zecca, M.B.H. Youdim, P. Riederer, J.R. Connor and R.R. Crichton, Iron, brain ageing and neurodegenerative disorders. *Nat. Rev. Neurosci.* **5** (2004) 863–873.

[32] J. Zhong, R.P. Kennan and J.C. Gore, Effects of susceptibility variations on NMR measurements of diffusion. *J. Magn. Reson. (1969)* **95** (1991) 267–280.